processes

MDPI

Review

A Review of Fabrication Methods, Properties and Applications of Superhydrophobic Metals

Kosmas Ellinas [1,*], Panagiotis Dimitrakellis [1,*,†], Panagiotis Sarkiris [1,2] and Evangelos Gogolides [1]

[1] Institute of Nanoscience and Nanotechnology, NCSR "Demokritos", Aghia Paraskevi, 15341 Attica, Greece; p.sarkiris@inn.demokritos.gr (P.S.); e.gogolides@inn.demokritos.gr (E.G.)
[2] School of Mechanical Engineering, National Technical University of Athens, Zografou, 15780 Attica, Greece
* Correspondence: k.ellinas@inn.demokritos.gr (K.E.); pdim@udel.edu (P.D.)
† Present address: Department of Chemical and Biomolecular Engineering, University of Delaware, Newark, DE 19716, USA.

Abstract: Hydrophobicity and superhydrophobicity with self-cleaning properties are well-known characteristics of several natural surfaces, such as the leaves of the sacred lotus plant (*Nelumbo nucifera*). To achieve a superhydrophobic state, micro- and nanometer scale topography should be realized on a low surface energy material, or a low surface energy coating should be deposited on top of the micro-nano topography if the material is inherently hydrophilic. Tailoring the surface chemistry and topography to control the wetting properties between extreme wetting states enables a palette of functionalities, such as self-cleaning, antifogging, anti-biofouling etc. A variety of surface topographies have been realized in polymers, ceramics, and metals. Metallic surfaces are particularly important in several engineering applications (e.g., naval, aircrafts, buildings, automobile) and their transformation to superhydrophobic can provide additional functionalities, such as corrosion protection, drag reduction, and anti-icing properties. This review paper focuses on the recent advances on superhydrophobic metals and alloys which can be applicable in real life applications and aims to provide an overview of the most promising methods to achieve sustainable superhydrophobicity.

Keywords: superhydrophobic; corrosion resistance; metals; wetting; nanotexturing

Citation: Ellinas, K.; Dimitrakellis, P.; Sarkiris, P.; Gogolides, E. A Review of Fabrication Methods, Properties and Applications of Superhydrophobic Metals. *Processes* **2021**, *9*, 666. https://doi.org/10.3390/pr9040666

Academic Editor: Monika Wawrzkiewicz

Received: 2 March 2021
Accepted: 6 April 2021
Published: 10 April 2021

1. Introduction

Water control at extreme states (i.e., superhydrophobicity or superhydrophilicity [1]), enables a palette of functionalities, such as self-cleaning, antifogging [2,3], anti-icing [4,5], anti-biofouling [6], high-binding [7], antibacterial activity [8–10], chemical shielding [11], drag reduction [12,13], etc. Wetting control has been achieved in a wide range of materials, such as polymers [14,15], metals [16,17], alloys [18], and ceramics using several fabrication methods [19–23].

For metallic substrates, besides corrosion, which is an extremely important issue for several applications of metals (i.e., naval, aircrafts, buildings, automobile), superhydrophobicity can enable additional functionalities such as anti-icing [24], dropwise condensation [25], frictionless motion, energy conversion [26], etc. Superhydrophobic interfaces in metals are typically prepared following two approaches (Figure 1). Following the first one, a hierarchical morphology is initially created on the metallic substrate by means of metal etching or oxidation (corrosion), and then the surface energy is minimized after the deposition of a thin hydrophobic layer. The low surface energy layer has to be thin enough not to alter the surface morphology, and simultaneously cover, effectively and homogenously, all morphology features to avoid defects and layer delamination. In the second approach, an organic, inorganic, or composite layer is deposited on a relatively smooth metallic substrate; this layer can be superhydrophobic or it can be transformed to superhydrophobic by creating appropriate morphology on its surface.

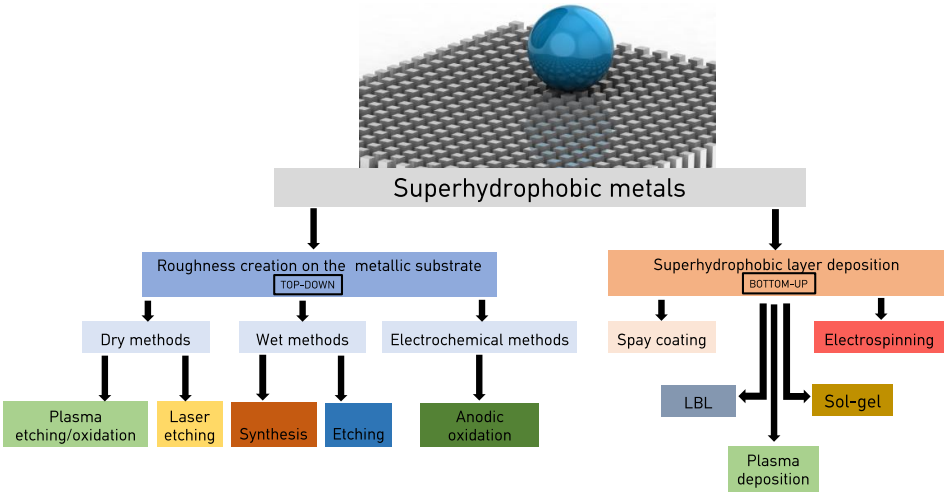

Figure 1. Overview of the fabrication methods used to transform metal surfaces to superhydrophobic. LBL: Layer by layer deposition.

There are several methods for the creation of surface morphology on metals that can lead to superhydrophobicity. These methods can be divided into wet methods (etching and synthesis), plasma methods (etching and synthesis), anodic oxidation, gas phase, and laser etching methods. Surface energy is usually reduced with the deposition of a hydrophobic, low surface energy coating. These coatings are deposited through dry methods, such as chemical vapor deposition (CVD) and plasma polymerization, or wet methods, such as immersion, spin coating, etc. The fabrication of superhydrophobic metallic surfaces after the deposition of a thick, low surface energy nanostructured layer on the metallic substrate can be achieved with several deposition methods, such as spray coating, electrospinning, electrodeposition, and sol–gel. An overview of the most common fabrication methods to transform metal surfaces to superhydrophobic ones is provided in Figure 1.

In our previous review papers we have discussed the advances in the fabrication of durable superhydrophobic and superoleophobic polymers incorporated in biomedical devices [15,27], as well as the superhydrophobic surface fabrication using atmospheric pressure cold plasma technology [28]. In addition, a wide range of reviews on superhydrophobic surfaces, coatings, and related applications can be found in the literature [18,19,29–31]. However, the review papers for superhydrophobicity in metals are limited [17,32,33] or are focused on one material, such as the recently published review paper for Magnesium (Mg) [34], or on one method, such as the review paper by Darmanin et al. about the electrochemical processes to fabricate superhydrophobic surfaces [35]. Thus, the information about the progress in this field is scattered and should be updated to include the new achievements and provide generic fabrication methods that are applicable for a wide range of metallic materials. Herein, we review the most common methods for superhydrophobic transformation of metals and alloys with great economic and industrial interest, such as aluminum, copper, magnesium, stainless steel, titanium, etc. These methods are put into context regarding their advantages and weaknesses. In addition, deterioration of metals due to corrosion is always a serious problem that needs to be resolved. Thus, the recent advances in corrosion protection using superhydrophobicity are also included. The durability of the proposed surfaces is also discussed and issues arising when superhydrophobic surfaces will be applied in real-life applications. Finally, we summarize the main findings and we provide some perspectives on the most promising approaches which can be adapted in real life for large-scale fabrication of durable superhydrophobic metals.

2. Theoretical Background of Wetting

Wetting control is determined by two factors: the surface chemistry and the surface topography. For an "ideal" completely smooth surface which follows the Young equation [36], the only determining factor is the surface chemistry (e.g., for a given surface, a

chemical modification can increase or decrease the surface energy and induce hydrophilic or hydrophobic properties respectively). The parameter that is used to assess the wettability of a solid surface is the water static contact angle (WSCA); a surface is considered hydrophobic if the WSCA is >90° and hydrophilic if WSCA < 90° [37]. An additional roughening step can enhance the wetting character of the surface and, starting from a hydrophilic material, WSCA can be reduced to <10° (superhydrophilic) or to reach high WSCA values >150° and become superhydrophobic [38,39]. However, WSCA by itself is not sufficient to fully characterize the surface wetting properties, it should be accompanied by dynamic contact angle measurements such as sliding angle, hysteresis or roll-off angle. Indeed for a surface to be characterized as superhydrophobic, sliding angle or contact angle hysteresis should be lower than 10° [40,41]. At these extreme non-wetting state, well described by the Cassie-Baxter model, the surface exhibits non-sticking and roll off behavior of water droplets, due to the microscopic air pockets entrapped between the water droplet and the surface protrusions, similar to those found in nature in the lotus leaf (*Nelumbo nucifera*) [42]. It is worth noting that besides the smooth hydrophobic and the rough superhydrophobic surfaces, there are also rough hydrophobic surfaces with high sliding or hysteresis angles, in which the water droplets stick and cannot roll off. Such wetting states (i.e., water wets the rough elements of the surface surfaces) lead to WSCAs in the range 100° < WSCA < 150° and sliding angles much higher than 10° that are described by the Wenzel model. Nevertheless, intermediate states as well as sticky surfaces with WSCA > 150° also exist, such as the rose petal, which is highly hydrophobic and sticky at the same time [43]. In Figure 2, a schematic representation of the different wetting states for a rough surface is presented.

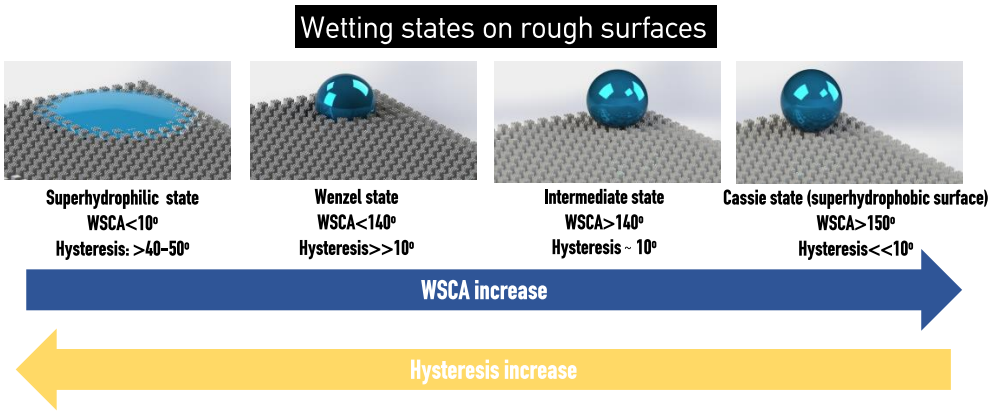

Figure 2. Wetting states of rough surfaces and respective wetting characteristics (WSCA and hysteresis).

3. Metal Superhydrophobicity via Creation of Hierarchical Morphology on Metallic Substrates

3.1. Wet Methods

Wet methods are commonly used to create the proper surface roughness on a metallic surface through treatment with a "harsh" chemical etching agent; that could be a strong acid such as HCl [44,45], a strong base such as NaOH [46], or even boiling water [47]. The roughening step is followed by the deposition of a low surface energy layer, such as polytetrafluoroethylene (PTFE) or other fluorinated compounds. Wet methods are categorized in (a) subtraction methods (etching with $FeCl_2$, HCl, etc.), as well as (b) synthesis methods (boehmitage process, hydrothermal synthesis) using boiling water.

3.1.1. Subtraction Methods

Several examples using iron (III) chloride ($FeCl_3$) to modify the aluminum substrate are available in the literature. For example, Maitra et al. [48] presented superhydrophobic surfaces with durability against solvents and mechanical stresses, and droplet impalement resistance after the deposition of a different hydrophobic layers (i.e., self-assembled monolayers, thin films, or nanofibrous coatings) on aluminum surfaces hierarchically textured

with $FeCl_3$. The same group used such surfaces for dropwise condensation targeting heat transfer applications [49]. J. Song et al. [50] used an aqueous copper (II) chloride ($CuCl_2$) solution to create roughness on aluminum followed by fluoroalkylsilane (FAS) modification.

In another report, superhydrophobic aluminum surfaces were fabricated by combination of chemical etching and fluorosilane coating using three different etching reagents, namely $AlCl_3$ (aluminum chloride), $FeCl_3$ and $CuCl_2$. This work highlights that, although all surfaces became superhydrophobic after fluorooctyltrichlorosilane (FOTS) deposition, the resulting topography is affected by the reagent used [51] (Figure 3).

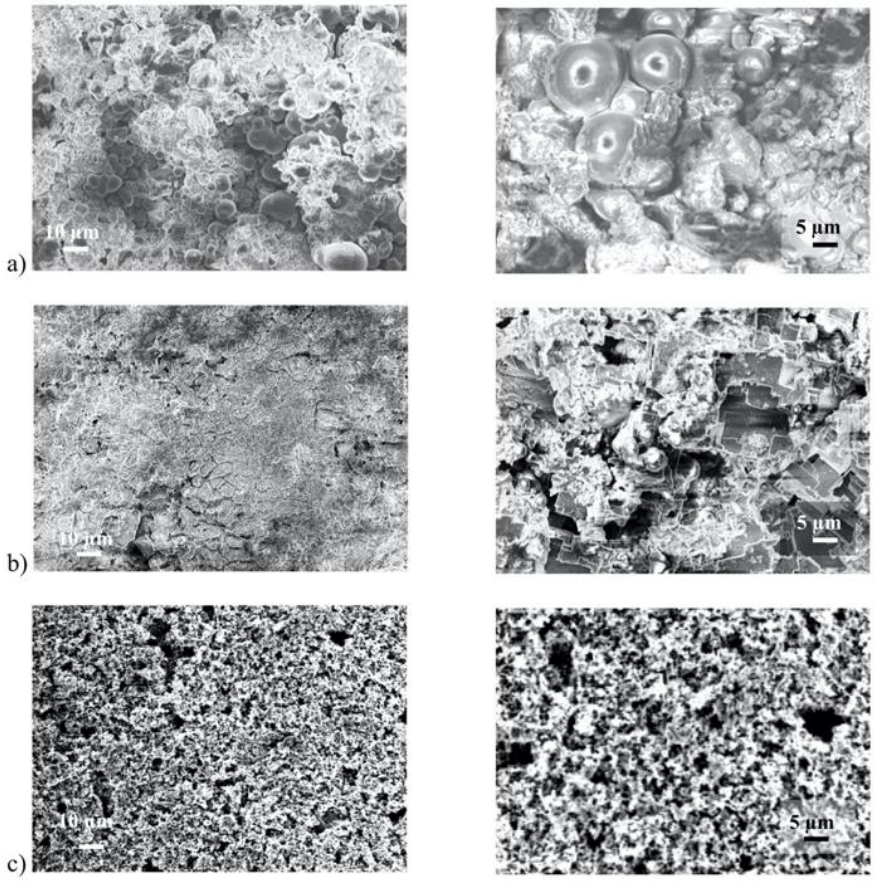

Figure 3. SEM images of textured aluminum: (**a**) Sample #1 after immersion in $AlCl_3$, (**b**) sample #2 after immersion in $FeCl_3$, and (**c**) sample #3 after immersion in $CuCl_2$ after the FOTS deposition. Reproduced with permission from [51].

Saleema et al. [46], on the other hand, used sodium hydroxide (NaOH) for etching and fluoroalkylsilane (FAS-17, $C_{16}H_{19}F_{17}O_3Si$)) for the surface modification of the etched Al surface, and reported the fabrication of superhydrophobic surfaces on aluminum alloy AA6061. The surfaces exhibited WSCA ~162° and very low contact angle hysteresis (~4°). An alternative two-step method based on the fabrication of a superamphiphobic polytetrafluoroethylene (PTFE)/cupric oxide (CuO) coating on 6061 aluminum was proposed by Zhexin Lv et al. [52]. They used sanding and etching in NaOH followed by immersion inside a 60% PTFE emulsion containing $CuSO_4$ and NaCl and a final thermal curing step at 380 °C for 30 min to fabricate superamphiphobic PTFE/CuO surfaces. The authors reported repellency against many liquids, including acidic and alkaline solutions, as well as enhanced corrosion resistance.

Hydrochloric acid (HCl) is another common reagent for etching of aluminum and other metals. Characteristic is the work of Chen et al. [53], who demonstrated superhydrophobic aluminum and zinc surfaces with stability against both acidic and alkaline conditions, as the WSCA retained its value above 150° without apparent fluctuation for

water droplets with pH value 1–14. The surfaces after the HCl etching were modified using 2.0 wt% fluoroalkylsilane FAS and exhibited improved corrosion resistance. Corresponding topographies after immersion in HCl for different times are shown in the SEM images presented in Figure 4.

Large-area, superhydrophobic copper surfaces were obtained via a replacement reaction between the substrate and a chloroauric acid ($HAuCl_4$) solution. The surface exhibited WSCA higher than 150° without addition of a hydrophobic coating [54]. Textured copper surfaces were also fabricated after immersion in ferric chloride ($FeCl_3$) solutions for different duration and solution concentration [55]. All surfaces exhibited a maximum WSCA of 140° and high sliding angle, but after modification using stearic acid, the contact angle increased to 150° and the sliding angle became lower than 10° in some cases. Another example is the work by Liu et al. [56], in which a solution-based procedure was applied; aluminum foils were immersed in an aqueous solution of $AlCl_3$ and triethanolamine (TEA) and the solution was heated at 100 °C for 5 h. The resulting boehmite film exhibited dual scale micro-nanotopography (Figure 4ii). The surface was finally modified after immersion in an ethanol solution of stearic acid (STA) for 10 h, leading to superhydrophobic properties, as evidenced by a WSCA of 169° and a sliding angle of ~4°.

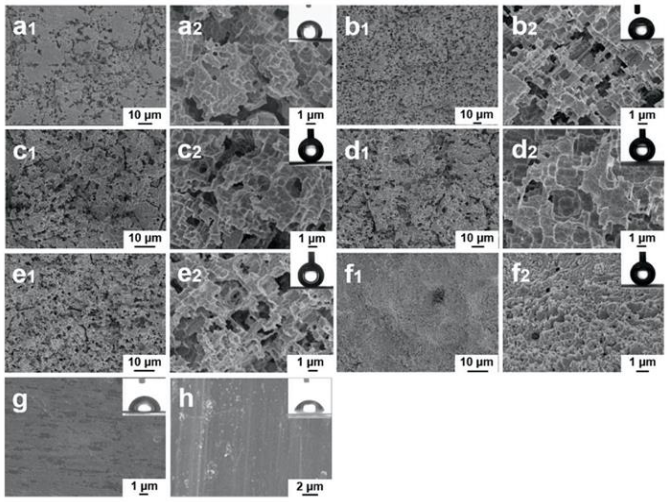

(**i**)

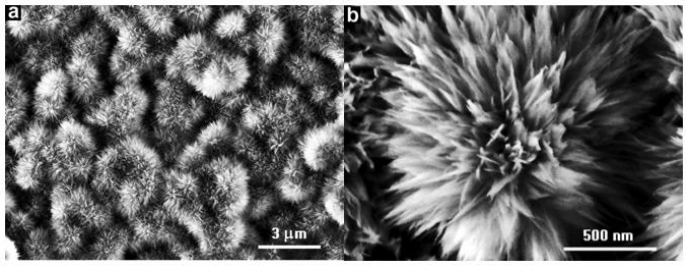

(**ii**)

Figure 4. (**i**) SEM images of Al after immersion in HCl for (**a1**,**a2**) 15 min, (**b**$_1$,**b**$_2$) 30 min, (**c**$_1$,**c**$_2$) 60 min, (**d**$_1$,**d**$_2$)75 min, and (**e**$_1$,**e**$_2$) 90 min respectively. (**f**$_1$,**f**$_2$) SEM images of Zn after immersion for 75 min. (**g**,**h**) The bare Al and Zn surfaces before etching. Reproduced with permission from [53]. (**ii**) SEM images of the resulting boehmite film on the aluminum foil prepared after immersing in a heated aqueous solution of aluminum chloride ($AlCl_3$) and triethanolamine (TEA). Reproduced with permission from [56].

In another recent work, Al plates were transformed to superhydrophobic after wet etching with HCl and deposition of FOTS (fluoroctatrichlorosilane). The surface anti-icing properties were evaluated exhibiting low ice adhesion strength and longer freezing time [57].

Therefore, the reagent used for the etching process influences the topography created and seems also to affect the adhesion quality of the hydrophobic coating used for hydrophobization.

In conclusion, wet etching is an efficient method to create hierarchical topography on metallic substrates, however the utilization of reagents with severe environmental footprint can make this technology less attractive to some applications. However, this technology is generic and can be applied in almost any metal material. For example, Al can be etched by $FeCl_3$, HCl or $CuCl_2$ solution. Stainless steel can be etched by a mixture of $FeCl_3$, HCl, H_3PO_4, and H_2O_2 and Mg alloys can be etched using an aqueous solution of $CuSO_4$ [58].

3.1.2. Synthesis Wet Methods

The treatment of aluminum in a boiling water can lead to the "growth" of hierarchical boehmite film on aluminum foils. One representative work of this method is the work by Jafari et al. [47], who reported a simple approach to fabricate a superhydrophobic surface after immersing Al in boiling water and subsequent sputtering of polytetrafluoroethylene (PTFE). They reported that the duration of the immersion step is critical for the resulting surface morphology (e.g., topography shifts from a "flower-like" structure in the first few minutes of immersion to a "cornflake" structure if immersion time was increased). A hot water treatment was also used for the formation of nanofeatures (Figure 5) in another example followed again by a hydrophobization step using perfluorooctyltriethoxysilane (POTS) [24].

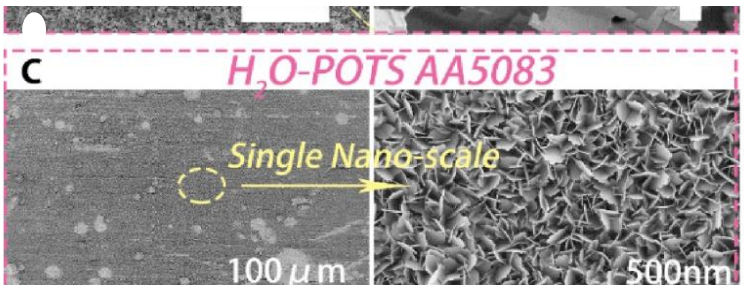

Figure 5. SEM images of aluminum substrates after immersion in boiling water and hydrophobization. Reproduced with permission from [24].

A hydrothermal method was used to compose a superhydrophobic coating of CeO2 and cerium stearate ($Ce(CH_3(CH_2)_{16}COO)_3$) on a Mg alloy. $Ce(CH_3(CH_2)_{16}COO)_3$ passivates the surface, leading to the formation of micro-nano hierarchical topography. The surfaces exhibited a high WSCA of 164° and a low rolling angle of 4°. The anticorrosion properties of the coating were evaluated using a 3.5 wt% NaCl aqueous solution. Authors reported two times lower corrosion compared to the bare Mg alloy, an improved performance which was attributed to the low contact area of the corrosion solution with the surface deriving from the superhydrophobic properties [59].

3.1.3. Combination of Wet Etching and Synthesis Method

In many cases, in order to create dual-scale, micro-nanostructures similar to those of lotus leaves, the combination of wet etching and immersion in boiling water has been reported [56]. As expected, Aluminum is widely used in such reports. A coral-like superhydrophobic surface with improved anti-icing performance was realized by combining chemical etching and hot-water treatment. The wet etching using HCl leads to the initial formation of micro scale roughness, while a second step using hot water leads to the formation of nano scale features (Figure 6i). Finally, a hydrophobization step was done using modification with 2 wt% hexadecyltrimethoxy silane. The prepared surface exhibited superhydrophobicity with a WSCA of ~165° and a sliding angle lower than 1°. Results also revealed that such coral-like superhydrophobic structures exhibit excellent anti-icing properties, as water droplets remained unfrozen at −6 °C for over 110 min. Moreover, 71% of the surface was free of ice when exposed in "glaze ice" for 30 min [24].

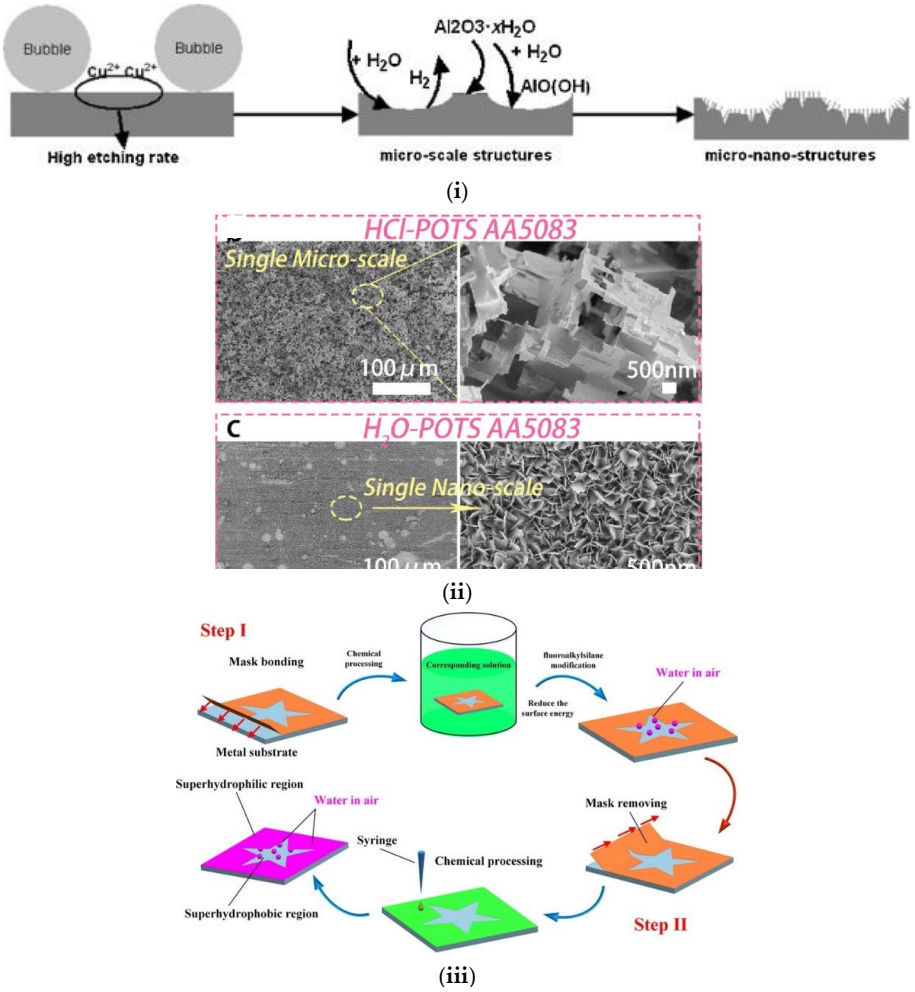

Figure 6. (**i**) Schematic illustration of fabrication micro-nano structures on aluminum used as anti-icing surfaces. Reproduced with permission from [24]. (**ii**) SEM images of superamphiphobic HCl-H_2O-POTS AA5083. Reproduced with permission from [60]. (**iii**) Fabrication process of different wettability patterns on the same surface. First, a superhydrophobic area is created using a mask based chemical processing and fluoroalkylsilane modification. Then, a superhydrophilic area is created by casting liquid drops. Reproduced with permission from [58].

In a similar work, superamphiphobicity was achieved also on aluminum by a multi-step process based on HCl etching (micro-roughness), H_2O treatment (nano-roughness), and perfluorooctyltriethoxysilane (POTS) grafting (hydrophobic finishing). After all steps were applied, the resulting surfaces exhibited micro-nano scale topography (Figure 6ii) and repelled liquids with surface tension down to 27.5 $mN{\cdot}m^{-1}$. In addition, stability against liquids with pH values ranging from 1 to 14 was also observed and the superhydrophobic properties were retained after 20 self-cleaning tests [60].

A mask-assisted method has been also proposed to prepare both superhydrophilic and superhydrophobic patterns on five kinds of metal substrates (i.e., aluminum, titanium, stainless steel, zinc and magnesium alloy), in order to highlight the versatility of the method. In particularly, Al was etched by 1 mol L^{-1} aqueous $CuCl_2$ solution. The 304 stainless steel was chemically etched using a mixture of 21 wt% $FeCl_3$, 2 mL HCl, 2 mL H_3PO_4, and 2 mL H_2O_2. Ti was etched using a 72% H_2SO_4 solution, Zn was textured by a mixture of 0.1 mol L^{-1} H_2SO_4 and 0.2 mol L^{-1} $CuSO_4$, and finally roughness was created on the Mg alloy after immersion in a 0.2 mol L^{-1} aqueous $CuSO_4$ solution. The surfaces were assessed in dropwise condensation and fog harvesting and big differences in the harvesting efficiency on various metal surface patterns were observed [58]. A schematic representation of the proposed method is shown in Figure 6iii.

In another approach, micro and nanoscale topography was formed on aluminum plate by combining chemical etching and anodization. After a fluorination step, the surface became super-repellent against liquids with surface tension in the range 27.5–72 mN/m. Anodization duration affected the morphology and the wettability accordingly. The adhesion properties were evaluated using Scotch tape, whereas the mechanical durability of the surfaces was probed using hardness tests. The results showed that surfaces retained mechanical robustness with almost no damage on the film and also remained stable after long-term storage [61].

This method is widely utilized and many new papers are added every day in the literature. In a recent one, anodization and liquid-phase deposition with lauric acid are combined to achieve superhydrophobicity and simultaneous superoleophilicity on Al exhibiting anticorrosion properties, while it was also reported that such surfaces if used underwater could remove microplastic particles [62].

3.2. Oxidation

Copper oxidation creates micro/nano-structures that can lead to superhydrophobicity. One example is the work by Lv et al. [63] in which a superhydrophobic CuO coating was fabricated by direct thermal oxidation of Cu on Al substrate, followed by a low-energy coating deposition using stearic acid (Figure 7i). This work is the follow up work from [52]. The resulting coating was superhydrophobic with WSCA and sliding angle of ~157 and ~4, respectively. Interestingly, the coatings retained the superhydrophobicity after several mechanical stresses (tape-peeling and sandpaper-abrasion) as well as chemical stability tests and exhibited improved anticorrosion properties.

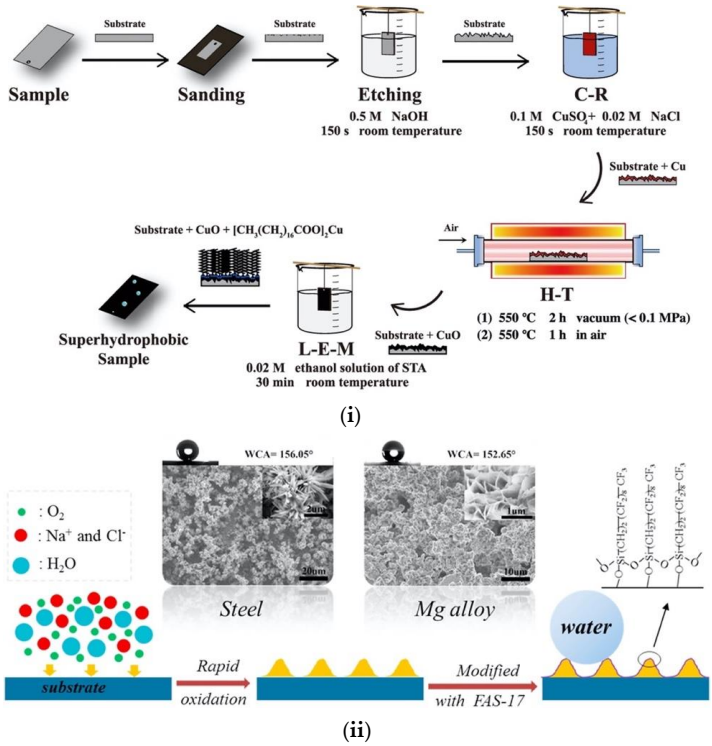

Figure 7. (**i**) The process flow for the leaf-like superhydrophobic coating. Reproduced with permission from [63]. (**ii**) Schematic representation of the method to fabricate superhydrophobic surfaces on steel and AZ31B magnesium alloy, as presented by Li Wang et al. [64]. SEM images of the topography created in both substrates are also provided as insets. Reproduced with permission from [64].

Another study reported an environmentally friendly oxidation method to fabricate superhydrophobic surfaces on stainless steel and magnesium alloy via salt spray and surface modification using FAS-17 [64] (Figure 7ii). They reported that hierarchi-

cal micro/nanometer-scale structures were induced in both metallic surfaces by electrochemical reactions during salt spray. The superhydrophobic surfaces showed remarkable durability, as evidenced by waterfall/jet tests.

3.3. Plasma Oxidation

Plasma oxidation is gaining attention as a tool for nano-fabrication due to the fast growth of high quality and purity materials of enhanced performance. For example, metal foils were converted to metal oxide nanowires when oxidized using weakly ionized, highly dissociated oxygen plasmas in an inductively coupled RF system [65]. Uniform growth of copper oxide nanowires has been also demonstrated after 10 min exposure to RF plasma discharges. In particular, copper samples of 20 mm diameter and 1 mm thickness were exposed to argon-oxygen plasma created at discharge power of 150 W. A theoretical model was also developed to explain the dependence of the nanowire length from the plasma parameters. They also explained that ballistic effects of ions and distortion of their local fluxes are limiting the nanowire growth [66]. Careful design of plasma grown metal oxide structures can lead to superhydrophobic surface fabrication upon deposition of a low surface energy layer.

In another work, E. Lee and K. Lee fabricated superhydrophobic steel surfaces by developing nanostructures through microwave spark irradiation under CO_2 atmosphere. The oxidation caused by microwave irradiation leads to volume expansion, which is the driving force of nano-structure creation. The hierarchical structures developed by the growth of nanostructures on the striped patterns of surface originating from the production process of the steel sheet, make the surface superhydrophobic, after coated with ODTS, with CA > 160° and hysteresis ~4°. The fabricated surfaces maintained superhydrophobicity after 14 days immersed in 5 wt% NaCl solution, proving their corrosion resistance [67].

Stainless steel Sus 304 was transformed to superhydrophobic exhibiting hierarchical topography and WSCA higher than 169° after combining microwave irradiation in CO_2 environment and chemical modification with a solution containing toluene and octadecyltetrachlorosilane (ODTS). The authors also reported stability against immersion inside a NaCl solution for a period reaching two weeks [67].

3.4. Laser Etching

Superhydrophobic metal alloy surfaces are important for aerospace and naval applications and can be used as anti-icing, antifogging, drag reduction, self-cleaning, and high-efficient light absorption surfaces. Moreover, stainless steel is widely used in architecture, industrial establishments, and medical instruments.

Laser etching can provide dual scale hierarchical structures on such surfaces and induce superhydrophobicity, as described in some recent review papers [22,68]. Moreover, laser-based surface texturing is considered as a precise and flexible method and several examples exist in the literature. For example, Kietzig et al. [16] created dual-scale rough structures by femtosecond laser irradiation on different metal alloys, which were transformed from superhydrophilic to superhydrophobic after 30 days of storage. Another interesting example is the nanosecond laser-based, high-throughput, two-step surface nanostructuring process used for superhydrophobicity [69]. During the first step, a high energy nanosecond pulse laser scans a metal surface which is submerged in water. After that, the laser-textured surface is hydrophobized by immersion in a hydrophobic chlorosilane reagent. After these two steps, the stainless steel surface exhibits micro- nano-scale features and a high WSCA even after using different laser power intensities (Figure 8).

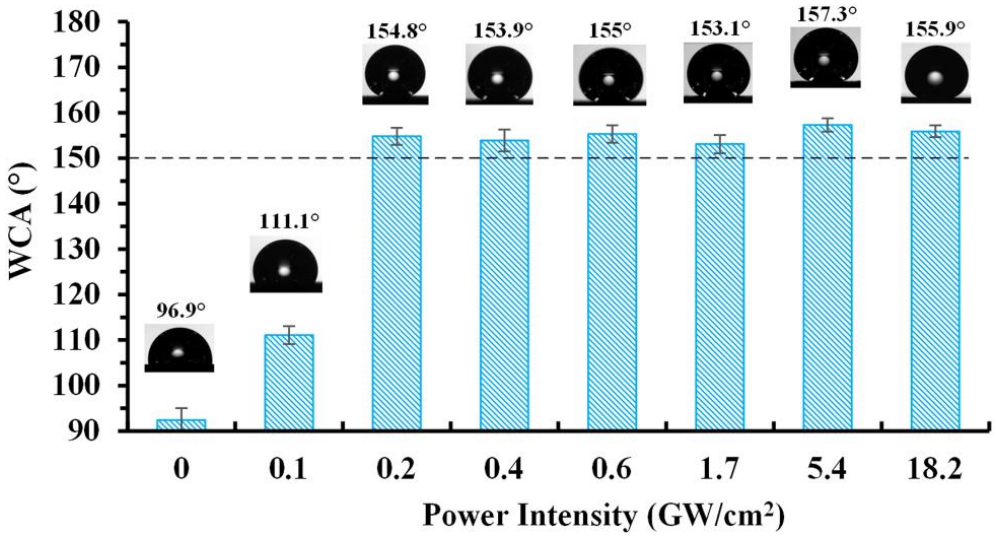

Figure 8. Contact angle variation of AISI 4130 stainless steel specimens produced at various laser power intensities. Reproduced with permission from [69].

In another work, laser processing was used to fabricate superhydrophobic surface on aluminum substrates [70]. They used a picosecond laser system due to the lower thermal effect on the aluminum substrate and created tilted groove patterns of various angles. Among the critical laser parameters, they reported that hatching distance (HD) and scanning speed (SS) were varied, while laser power was kept constant. The surfaces were initially superhydrophilic and they were transformed to superhydrophobic after 15 days of storage in ambient conditions.

Laser etching was also used by Sharjeel A. Khan et al. to fabricate superhydrophobic surfaces on Al, Cu, and galvanized steel. The authors instead of depositing a low surface energy coating they proposed the use of ageing in a low-pressure environment that can transform the surfaces to superhydrophobic in just 6 h. They also studied the effect of the pulse duration (by using femtosecond and picosecond pulse durations) as well as the scanning speed [71].

Laser etching was combined with spraying of a solution containing a nonionic fluorinated surfactant (FS-61), ethanol and PTFE nanoparticles for the creation of superamphiphobic surfaces exhibiting hierarchical micro-nano topography on Al and Steel. The surfaces repelled water and other liquids, such as ethylene glycol, rapeseed oil, and cyclohexane, and exhibited antifouling properties and good mechanical durability against abrasion [72].

3.5. Electrodeposition

Corrosion is one of the most challenging issues for the magnesium alloys; therefore, transforming Mg alloys to superhydrophobic is crucial for their effective anticorrosion protection. To this direction, Zhang et al. [73] proposed the application of a textured ceria (CeO_2)/stearic acid bilayer coating on top of AZ31B Mg substrates. They used a simple electrodeposition method to prepare petal-like, hierarchical CeO_2 nanosheets, followed by immersion in stearic acid solution as the hydrophobic finishing step (Figure 9i). The optimum conditions were realized for 60 min total electrodeposition time, combined with 0.65 mA/cm^2 current density. The resulting coating exhibited good superhydrophobic properties with WSCA > 158° and sliding angle < 2°, while the anti-corrosion performance in 3.5 wt% NaCl solution was significantly improved.

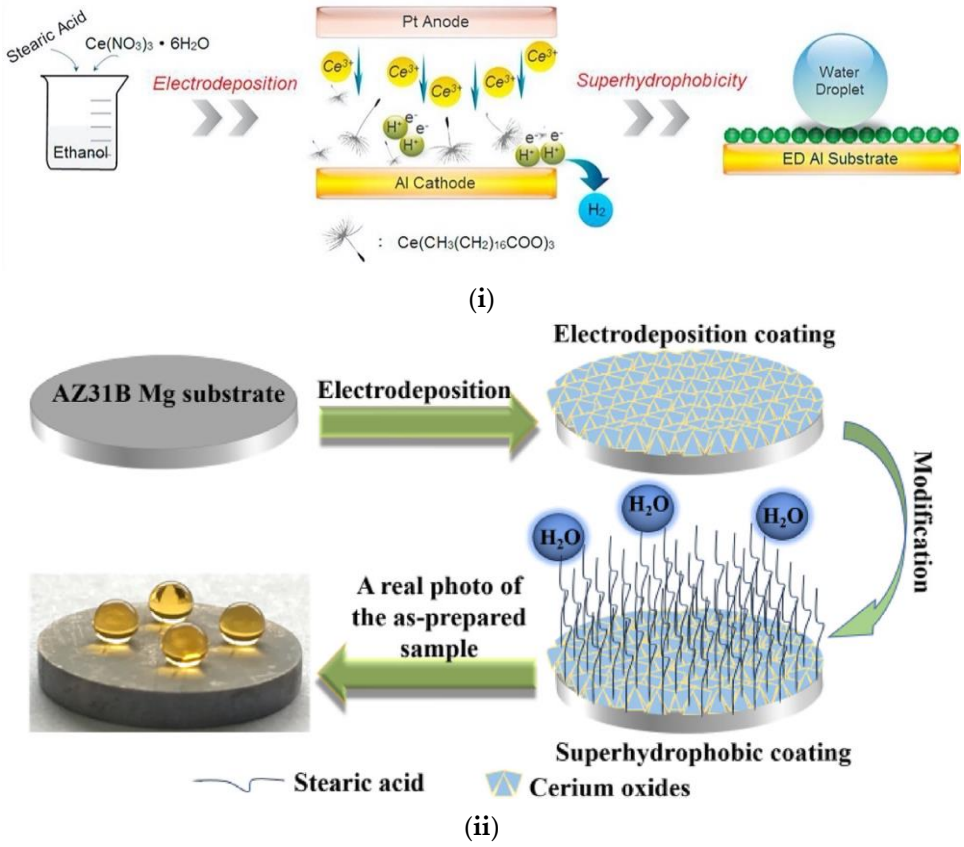

Figure 9. (**i**) Schematic representation of the fabrication method, as described by Binbin Zhang et al. [73]. Reproduced with permission from [73]. (**ii**) Schematic diagram of preparation process of the superhydrophobic coating formed on the AZ31B Mg substrate. Reproduced with permission from [74].

In another example, nonfluorinated superhydrophobic Al surfaces were prepared via one-step electrodeposition method. The authors used air-exposure and 3.5 wt% NaCl immersion tests to evaluate the quality of the surface (Figure 9ii) [74].

Taking advantage of the stability and penetrability of layer-by-layer (LbL) films, Ag aggregates were incorporated inside the matrix of a LbL polyelectrolyte multilayer deposited on Indium tin oxide (ITO) [75]. The morphology of Ag aggregates was adjusted by tuning time and potential. The surface became superhydrophobic with a WSCA: 154° and a tilt angle lower than 3°.

In a recently published paper by Zihao He et al., aluminum chloride hexahydrate and N-dodecyltrimethoxysilane (DTMS) in ethanol was used as electrolyte solution for the fabrication of a superhydrophobic surface with WSCA 155° and 99.9% corrosion resistance when immersed inside a 3.5 wt% NaCl solution. This excellent anticorrosion behavior remained above 98% even after 30 days of immersion [76].

4. Superhydrophobicity after Deposition of a Polymeric or Composite Layer on the Metal Substrate

Due to the great demand of metals for industrial, structural, as well as construction applications, their protection and durability especially in marine environments is extremely important and has attracted a lot of interest from the scientific community. A commonly used approach to prolong the service life of metal structures is to apply organic coatings to avoid corrosion and other degradation phenomena [77,78]. In this section we will present the most promising methods to deposit such coatings on metals as well as their applications.

4.1. Plasma Polymerized Coatings

Plasma processing is a widely used technique for surface modification of materials; among its advantages are the high versatility and controllability and its environmentally friendly character as it is a "dry: technique based only on (gaseous) plasma–(solid) surface interactions. Plasmas, the so-called "fourth state of matter", are highly reactive media comprising a complex chemistry, rich in reactive species such as radicals, atoms, molecules, positive and negative ions, electrons, and photons.

Plasma surface nanoengineering towards fabrication of superhydrophobic surfaces has been studied extensively during the last decades. Several approaches have been proposed using either thermal or non-thermal plasmas, low or atmospheric pressure, and several plasma reactor configurations. Different nanostructured, low-surface energy materials have been proposed as well and the targeted functionalized surfaces range from plastics and composites to glass and metals [79,80].

Fabrication of superhydrophobic metallic surfaces via deposition of plasma-polymer coatings is enabled using plasmas far from thermal equilibrium (cold plasmas); the surface temperature during plasma treatment is a few hundred Kelvin and even close to ambient, thus facilitating the formation of well-defined hierarchical structures from organic, heat-sensitive materials. Most of the works related to deposition of superhydrophobic organic coatings on metals are dealing with atmospheric pressure plasmas, where the high-pressure operation and high precursor concentrations facilitate the rapid texturing of the surface, contrary to low-pressure plasmas where the deposited coatings are typically smooth and conformal.

The most frequently applied precursors for deposition of plasma-polymerized coatings on metals are organosilicon molecules that lead to plasma-polymers with a siloxane -Si-O-Si- backbone and hydrophobic -CH_3 side groups [28]. Figure 10i provides an overview of some of the precursor molecules proposed for deposition of hydrophobic and superhydrophobic coatings.

Among the different approaches on the plasma processing itself is the direct (single-step) deposition of micro-nanostructured and low surface energy coatings on a relatively smooth metal substrate. Early efforts focused on low-pressure plasma polymerization of organosilicon precursors. Grundmeier et al. [81] applied low-pressure microwave plasma to deposit superhydrophobic coatings on electrogalvanized steel (EGS). They applied Ar/HMDS discharges and deposited plasma-polymerized organosilicon coatings that were rich in hydrophobic methyl groups and exhibited micro-nanoscale roughness due to the formation of particles. The measured static WSCA was up to 160°. Ishizaki et al. [82] also applied microwave plasma using trimethylmethoxysilane (TMMOS) precursor in Ar carrier gas and deposited superhydrophobic coatings on magnesium alloy AZ31. They observed the formation of micro-nano roughness on the plasma-polymerized coatings for prolonged deposition times; after 20 min deposition the coatings were superhydrophobic with WSCAs higher than 150° (Figure 10ii). It is worth noting that the superhydrophobic metallic substrates exhibited high anticorrosion resistance, as deduced from electrochemical impedance spectroscopy (EIS) measurements, and also high chemical stability in neutral and acidic environments.

Atmospheric pressure plasmas have also been proposed for fast deposition of water-repellent coatings. Beck et al. [83] used a dielectric barrier discharge (DBD) jet operating in atmospheric pressure with mixtures of He/octamethylcyclotetrasiloxane (OMCTS). They deposited powdery superhydrophobic coatings with a WSCA of around 160° on electro chromium-coated steel (ECCS). Kim et al. [84] proposed the deposition of soft superhydrophobic films on stainless-steel plates using atmospheric pressure DBD plasma in filamentary mode. The precursor was hexamethylcyclotrisiloxane (HMCTSO) in N_2 carrier gas and the deposited coating exhibited dual-scale topography and WSCA = 162°. In the above works the contact angle hysteresis is not presented.

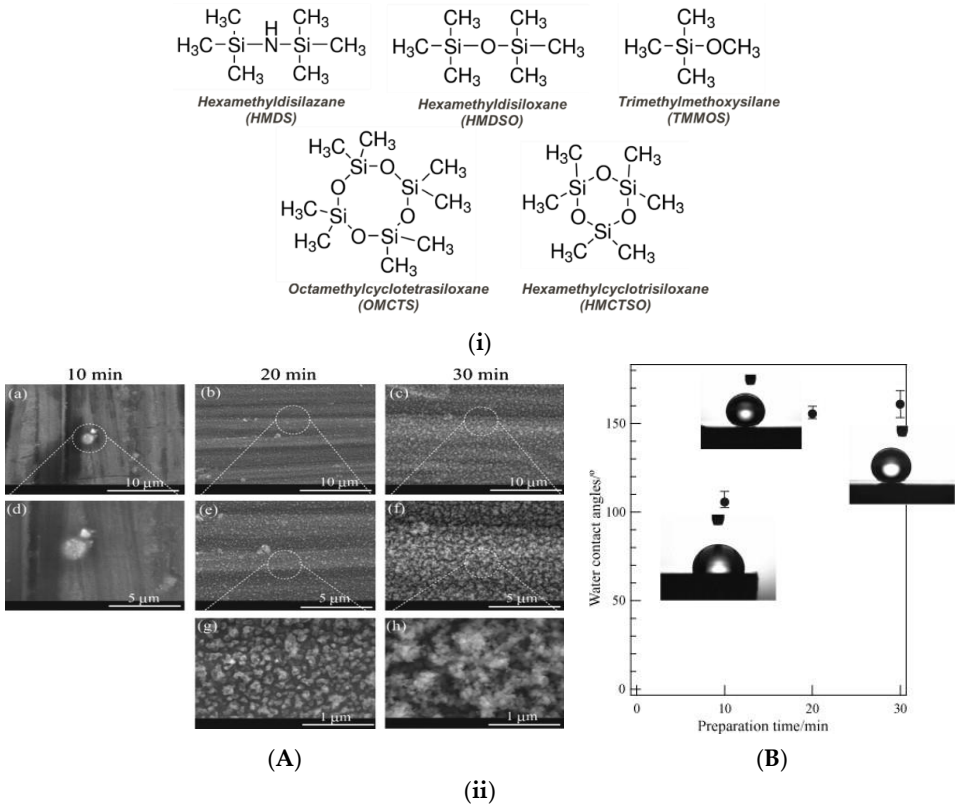

Figure 10. (**i**) Most common organosilicon precursors for the single-step deposition of plasma-polymerized superhydrophobic coatings either in low or atmospheric pressure. (**ii**) Microwave low-pressure plasma deposited coatings using a gas mixture containing trimethylmethoxysilane and Argon on magnesium alloy AZ31: (**A**) SEM images of the coatings and (**B**) water contact angle measurements for different plasma deposition times. Reproduced with permission from [82].

While the plasma deposition in atmospheric pressure is offering a facile and promising route towards continuous and large-area fabrication of micro-nanostructured superhydrophobic coatings, the single-step deposition can also easily lead to soft and powdery coatings; hence, the durability of superhydrophobic functionality remains questionable.

Another approach to improve durability in either low or atmospheric pressure plasma deposition is to follow dual-step processing, where a pre-roughening of the metal substrate in the micro-scale enables the fabrication of robust superhydrophobic surfaces after a subsequent deposition of a thin, plasma-polymerized, nano-rough coating. The pre-roughening of the metal substrate can be achieved via a palette of different methods; the reader could refer to the Section 2. In the following paragraph we review the main works related to the dual-step fabrication of superhydrophobic metals, where at least the second step entails the deposition of a plasma-polymerized hydrophobic coating.

Sarkar et al. [45] first created micro-nano roughness on aluminum by chemical etching using hydrochloric acid (HCl), and next they applied the deposition of a low-pressure plasma-polymerized thin film of low surface energy. They used mixtures of Ar with CH_4 and C_2F_6 and they managed the deposition of fluorinated hydrocarbon coatings with a high fluorine content around 36%. The hydrophobic coatings were smooth and yielded a WSCA of 105° on a smooth silicon surface; however, the deposition on the pre-roughened aluminum resulted in roll-off superhydrophobicity, as evidenced by a high static WSCA of around 165° and low contact angle hysteresis of 2°.

Mobarakeh et al. [85] used the same low-pressure plasma device, namely an RF 13.56 MHz driven inductively coupled plasma reactor, and deposited plasma-polymerized organosilicon thin films from Ar/HMDSO discharges on aluminum substrates. The aluminum alloy samples had previously been anodized and the deposition of the hydrophobic

coating resulted in superhydrophobic behavior with WSCA of 162°. The wettability of the untreated, anodized, and plasma-deposited aluminum is shown in Figure 11. The durability of the superhydrophobic aluminum surfaces was assessed through successive icing–de-icing cycles, UV exposure, anticorrosion resistance and immersion in DI water. After 15 icing–de-icing cycles the surfaces retained the hierarchical morphology and the icephobic properties, the coatings were resistant to UV exposure up to 537 h and the anticorrosion resistance was improved up to 16 times; upon prolonged immersion in pure water the surfaces gradually lost their superhydrophobic character, with the WSCA decreasing down to 120° after 1000 h.

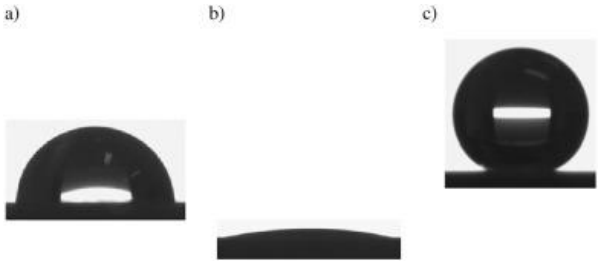

Figure 11. Wettability of (**a**) untreated, (**b**) anodized, and (**c**) superhydrophobic aluminum after low-pressure deposition of a plasma-polymerized hydrophobic coating from Ar/HMDSO discharges. Reproduced with permission from [85].

In another work, Boscher et al. [86] proposed the fabrication of superhydrophobic surfaces on cold-rolled aluminum foil using DBD plasma in atmospheric pressure. The plasma device operated in N_2/HMDSO gas mixtures and was able for continuous processing (Figure 12). The rose petal (sticky) superhydrophobic properties were attributed to the insufficient micro-scale roughness of the aluminum substrate. In the follow-up work, they focused on the optimization of surface topography prior to plasma polymerization step and they managed a roll-off superhydrophobic behavior on cold-rolled aluminum foils and electrodeposited copper foils [87]. The combination (dual-step process) of appropriate surface finishing and plasma deposition of nanorough organosilicon (hydrophobic) coating resulted in high static WSCA (170°) and low contact angle hysteresis (5°). The surfaces retained their superhydrophobic behavior upon storage in air or immersion in water even after six months.

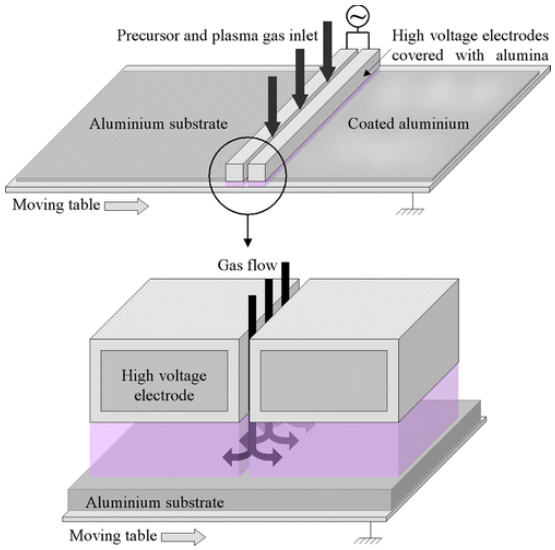

Figure 12. Schematic of an atmospheric pressure dielectric barrier discharge (DBD) device for large-area deposition of plasma-polymerized organosilicon thin films. Reproduced with permission from [86].

Jafari et al. [88] proposed another route towards fabrication of superhydrophobic aluminum based on dual-step processing employing successive plasma treatments in atmospheric pressure. First, an air plasma treatment was applied to aluminum using a commercial plasma jet (PlasmaTreat) to induce initial roughness and, next, a rough organosilicon coating was deposited from N_2/HMDSO discharges using the same device. With increasing the number of passes from the HMDSO plasma, the deposited coating was grown thicker and with larger features. The plasma operation at low power and low flow rates could prevent the over-fragmentation of the precursor and the formation of powder. The optimum surfaces exhibited roll-off superhydrophobic behavior with static WSCA of 163° and hysteresis of 1°. The superhydrophobic surfaces were also durable for at least seven days when submerged into water, acid and base; icephobic properties could also be retained after successive icing–de-icing cycles.

4.2. Spray Coatings

Spray coating is a very simple technique and easy to implement in continuous, large-area processing; hence, it is widely applied for the fabrication of several kinds of coatings, among which are the hierarchical, superhydrophobic coatings on a range of substrates [89,90]. It is based on wet chemical methods to prepare a liquid solution or suspension, which in the case of superhydrophobic coatings are typically micro- or nanoparticles, functionalized with a low surface energy compound. In the case of metal substrates, that technique can prove very useful, as it can be generic to any kind of substrate and does not typically require any pre-roughening step.

An aluminum alloy was first chemically etched and then transformed to superhydrophobic using a spray coating of an alcohol solution containing hydrophobic silica nanoparticles (15–40 nm) and methyl silicate. The initial micro-roughness formed on aluminum, coupled with nano-scale, low surface energy particles, resulted in superhydrophobic properties, as evidenced by a WSCA of 155° and a roll-off angle of 4°. The coating was subjected to repeated mechanical tests, including high-pressure water jetting, sand particles impacting, and sandpaper shear abrasion. It retained its superhydrophobicity with a hysteresis < 10° up to three cycles of water jetting (25 kPa for 10 min) and sand particle impinging. After five cycles, the roll-off angle increased up to 19°, while the static WSCA remained above 150° (Figure 13i). The authors also reported that the topography created on Al by chemical etching enhanced the coating adhesion since the particles could adhere better on the rough Al [89].

In a similar work, the superhydrophobicity was achieved via a single-step spraying of copper substrate without pre-roughening of the metal surface. To do so, authors sprayed a solution silica nanoparticles grafted with octyltriethoxysilane to adhesive polymer. SEM images revealed the formation of a dual-scale roughness and WSCA measurements showed the fabrication of superhydrophobic surfaces, with WSCA 160° and sliding angle lower than 5° (Figure 13ii). The coatings were characterized by electrochemical impedance spectroscopy (EIS) and Tafel polarization curves. They reported good performance against corrosion in 3.5% NaCl solution and good adhesion on the copper substrate after applying ASTM D-3395 [91].

In another study, a so claimed super-robust, superhydrophobic composite coating with a maximum WSCA of 159° and a low sliding angle of 3.5° has been presented. The composite coating preparation method is presented in Figure 13iii and could be spray coated in various substrates. Briefly, montmorillonite (MMT) clay particles were initially incorporated in a polydimethylsiloxane (PDMS) network, which was then reacted with the carboxylic acid groups of polysulfone (PSU) and finally mixed with polyvinylidene fluoride (PVDF). The authors reported improved ductility and mechanical properties of the PSU composite due to the cross-linking ability of PVDF and the multilayer structure of MMT. In particular, they reported 14.3 times higher wear resistance when compared to a commercial fluorocarbon coating. Simultaneously, the prepared superhydrophobic coating also exhibited good corrosion resistance properties, since corrosion current density

and corrosion potential decreased from 100.9 to 103.6 mA/cm^2 and from 803 to 218 mV, respectively. The authors claim that the proposed fabrication scheme can enable large-scale fabrication and; therefore, such coatings can be adapted by the industry [92].

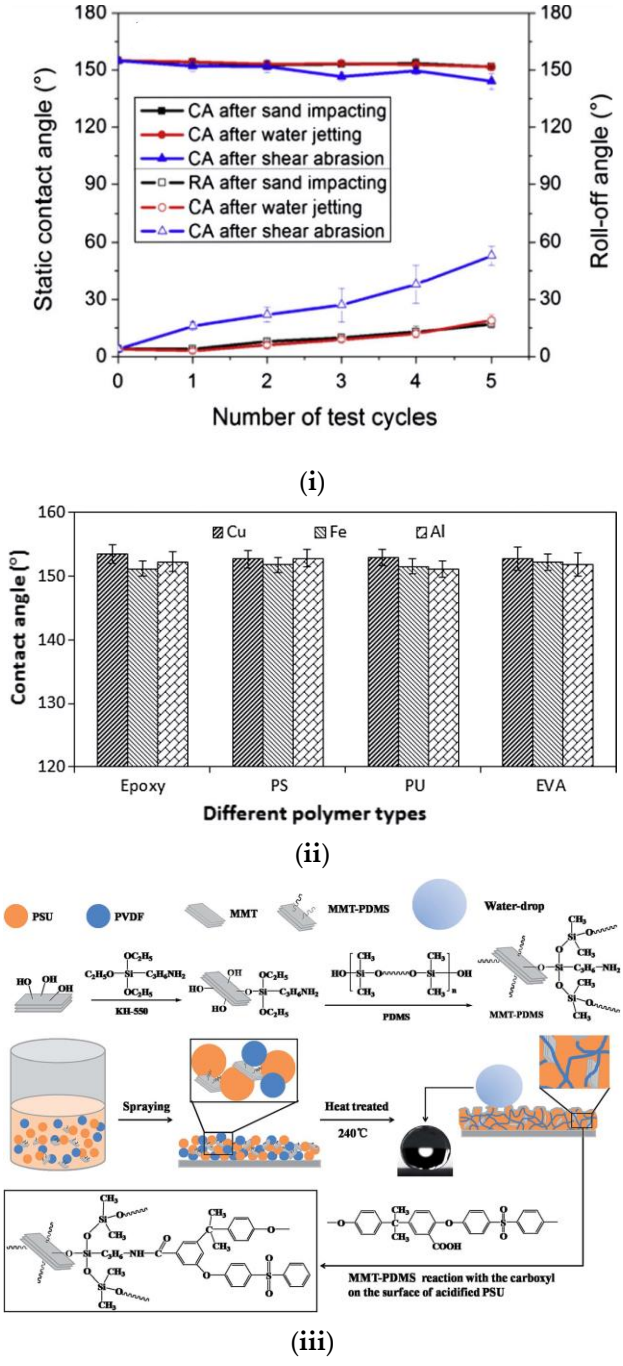

Figure 13. Spray coating of a superhydrophobic material. (**i**) Static and roll-off contact angles on functionalized silica nanoparticle coated etched aluminum alloy after repeated mechanical tests. In the water jetting tests, the samples were jetted at 25 kPa for 10 min. Reproduced with permission from [89]. (**ii**) The WSCA at optimum silica percentage (2.5 wt%) with optimum polymer percentage (2 wt%) using different polymer types at various metallic substrates. Reproduced with permission from [91]. (**iii**) Schematic representation of the preparation method of superhydrophobic polysulfone/polyvinylidene/montmorillonite/polydimethylsiloxane (PSU/PVDF/MMT-PDMS) composite coatings, as described by Wang et al. Reproduced with permission from [92].

Sprayable, superhydrophobic, nano-chain coatings were applied on copper substrates [93]. The surfaces exhibited continuous self-jumping of drops condensed on the surface, whereas on the coatings lacking nano-pores the dew drops only slipped under the effect of gravity.

A fluorine-free superhydrophobic coating with repairability and easy applicability using the spray coating technique has also been presented [94]. More specifically, superhydrophobic surfaces were prepared by spray-coating low-cost metal alkylcarboxylates (i.e., $Cu[CH_3(CH_2)_{10}COO]_2$) onto any substrate, as the authors claim. Superhydrophobicity with a WSCA of about 160° and a sliding angle of 5° was achieved at optimum conditions. The hydrophobic properties were dependent on the surface morphology, which in turn could be tuned by changing the precursor concentration. In particular, if the precursor concentration was low (0.02 M), the surface wetting properties followed the Wenzel model and all drops, even the ones gently deposited on the surface, stuck on it. On the contrary, when the concentration increased (0.04 M), coatings with dual roughness at both micro- and nanoscale were formed and a stable Cassie state was achieved.

As it clear from this section, this method, due to its simplicity, scalability, and cost-effectiveness, is well accepted by many researchers and can be applied on the large industrial scale. However, the adhesion of the coating with metal substrate can be problematic and ways to further improve its adhesion on the substrates should be developed.

4.3. Sputtering

Sputtering is another method that can be used for the deposition of a low surface energy coating on preformed topography. For example, in the work by Yang Wang et al. [95], a method of fabricating superhydrophobic surface on aluminum alloy substrate was presented. The etching of aluminum surfaces has been performed using dislocation etching for different duration and created micrometer-sized irregular patterns. The duration of 50 s was identified as the optimum duration for this step, followed by polytetrafluoroethylene (PTFE) coating sputtering. After PTFE sputtering, the surface exhibited a water contact angle of 165 $\pm$ 2° with a contact angle hysteresis as low as 5 $\pm$ 2°. Jafari et al. [47] also used sputtering of polytetrafluoroethylene (PTFE) for hydrophobization of the topography created after immersing Al substrates in boiling water, and reported high water contact angles and low hysteresis values.

4.4. Electrospinning

Electrospinning is another well-established technique to produce micro-nanofiber coatings for a wide range of applications. This technique is based on an electric force which draws charged parts of polymers to create fibers with diameters of some hundred nanometers [96,97].

In one of the reports, electrospinning of a solution containing tetrahydrofuran and dimethylformamide resulted in block copolymer poly(styrene-b-dimethylsiloxane) (PS-b-PDMS) fibers with diameters ranging from 150 to 400 nm. The fibrous surfaces were superhydrophobic, with WSCA 163° and contact angle hysteresis of 15°. The superhydrophobicity was attributed to the combination of surface enrichment in hydrophobic siloxane chemistry and the surface roughness of the electrospun mat itself [98]. In a follow-up work by the Gregory C. Rutledge's group, superhydrophobic fabric was produced by combining electrospinning and chemical vapor deposition (CVD) [99]. In this work, a correlation of the water contact angle with the fiber size and type was also presented (Figure 14).

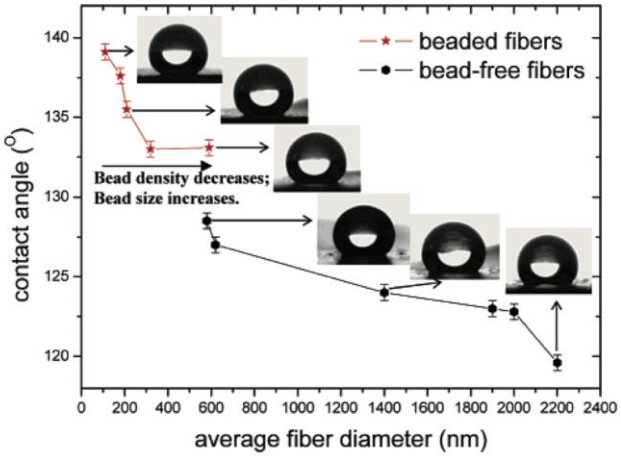

Figure 14. Contact angles for the as-spun poly(caprolactone) PCL mats. From bottom to top in the inset are representative droplet images on samples F1, F4, F6, B1, B3, and B5. The contact angles are 119°, 124°, 129°, 133°, 135°, and 139°, respectively. Reproduced with permission from [99].

Han et al. [100] presented some core−sheath structured micro-nanofibers that combine different properties deriving from the core and sheath materials using electrospinning. To do so, they used amorphous fluoropolymer (Teflon AF) and poly(ε-caprolactone) (PCL) as core materials. The resulting core–sheath fibers were used successfully for the fabrication of superhydrophobic and oleophobic membranes. The fibers preserved the core material properties after mechanical tensile tests. This approach is expected to provide new material combinations with many potential applications.

In another work, electrospinning was used to prepare hydrophobic and self-cleaning polysulfone (PSU) surfaces. By changing the PSU concentration in dimethylformamide (DMF) solvent, as well as the electrospinning process parameters, they demonstrated three types of morphologies (i.e., beads, beads-on-strings, and free-beads fibers). The contact angle (CA) increased to more than 160° for the electrospun fibers surfaces (from 73° for the smooth PSU surface) and in all cases contact angle hysteresis (CAH) was lower than 10°. The thickness of PSU mats could also be tuned from 10 to 70 μm [101].

Due to the versatility of this method, many papers reporting the fabrication of superhydrophobic coatings have been reported [102,103]. However, in most of these studies the durability of the proposed coatings is not discussed and it is; therefore, not clear whether this approach can provide durable coatings with good adhesion when deposited on metals.

4.5. Sol–Gel

Sol–gel is a wet, chemical method used for the creation of both glassy and ceramic materials. In this process, the sol (or solution) gradually turns into a gel-like network containing both a liquid phase and a solid phase. Inorganic–organic hybrid coatings on metals or alloys by the sol–gel process are promising for anti-corrosion applications [104]. Inorganic sols in hybrid coatings increase adhesion by forming chemical bonds between metals and hybrid coatings, and simultaneously improve the properties of the polymer. Incorporation of organic polymers with properties, such as hydrophobicity, increased cross-linking density, etc., enables the control of the resulting gel properties. For example, organic components of hybrid coatings with repellency to water can be used for corrosion protection of metals. A 1997 review describes the differences of ceramic coatings and sol–gels [105]. Nowadays, as reported above, several sol–gel protective coatings, with excellent chemical stability, oxidation control, and enhanced corrosion resistance for metal substrates, have been presented in the literature [106]. In this section we present below some representative examples of this approach.

One example of this method is the thermally stable and transparent superhydrophobic sol–gel coating deposited by spraying, as reported by Satish A. Mahadik et al. [107]. The coating was methyltriethoxysilane based and was transparent and superhydrophobic when

deposited on glass substrates. A surface modification process was applied using monofunctional 10% TMCS in the hexane bath. The coating also remained hydrophobic after thermal stress. Another example of the sol–gel methodology is the work presented by Shixiang Lu et al. [108].

Epoxy and polyurethane coatings exhibit inherently high surface energy. Thus, their performance against degradation is poor; to address this defect, nanostructured hydrophobic and superhydrophobic polysiloxane coatings have being proposed [109]. The coatings were prepared by sol–gel process using perfluorodecyltrichlorosilane (FDTS), nanoZnO particles, and poly(dimethylsiloxane) (PDMS). The coatings were evaluated for their liquid repellency, surface morphology, and roughness, as well as their electrochemical and salt spray corrosion. The results of this work showed that that anticorrosion performance was considerably dependent on the ratio of the nanoZnO particles and PDMS, and the optimum effect was observed for the superhydrophobic coating fabricated using ratio of 1:1. Such coatings can be used as marine coatings that can delay or even eliminate corrosion.

In the work of Zheng et al. [110], they studied important factors during the sol–gel process in order to optimize the anticorrosion performance of hybrid coatings. It was reported that electro-deposition results in thick, homogeneous, and defect-free hybrid coatings, in comparison to dip or spin coating techniques. Moreover, they found that green cerium ions and non-ionizable organic inhibitors can perform better in hybrid coatings compared to other corrosion inhibitors. They also studied the approach to encapsulate inhibitors inside the films to prolong the anticorrosive behavior. According to the authors, the ideal model of hybrid coating for superior anti-corrosion of metals is the combination of superhydrophobic hybrid coating and an underlying hybrid coating doped with corrosion inhibitors. In another work, superhydrophobic membranes with high roughness and chemical compositions were prepared by sol–gel method [111]. They reported that the surface morphology plays more important role in anti-corrosion ability in humid air (Figure 15).

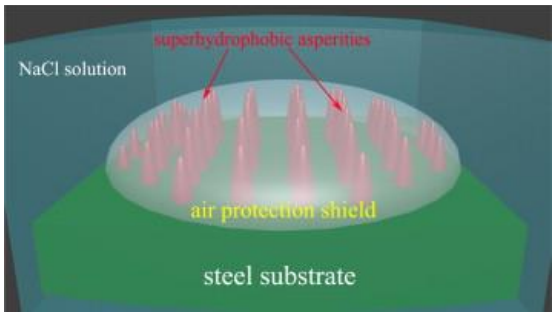

Figure 15. Representation of the anti-corrosion mechanism of superhydrophobic membranes in corrosive solution medium. Reproduced with permission from [111].

In another work, neutron reflectivity (NR) was used to study the performance of superhydrophobic films against corrosion. A low-temperature, low-pressure technique was used to prepare a rough, thin (~500 nm), nano-porous organosilica, aerogel-like film. Then, they applied UV exposure to control the surface coverage with hydrophobic organic ligands on the silica framework and identified an optimum surface exhibiting WSCA up to 160°. NR measurements showed that superhydrophobicity prevents water penetration into the porous film and thus limits the exposure of corrosive elements to the metal surface, in this case aluminum [112].

4.6. Layer-by-Layer Deposition

Layer-by-layer (LbL) deposition is a powerful tool for polymer surface modification [113] and has been employed in many reports in the literature [114,115]. Concerning the LbL deposition on metallic substrates, a representative work is the one by Syed et al. [116]. They proposed a layer-by-layer, spin-assembled coating, made of a polyaniline-silica composite, coupled with tetramethylsilane (TMS) functionalized silica nanoparticles (PSC/TMS-

SiO_2) (Figure 16). The composite coating was applied on 316 stainless steel and the TMS-SiO_2 content on the deposited coatings was optimized to achieve superhydrophobic properties, as evidenced by high WSCA of 153° and small sliding angle of 6°. They also reported a significantly enhanced corrosion resistance, which remained stable even after 240 h of exposure to 3.5% NaCl solution, attributed mainly to the superhydrophobic properties of the coating.

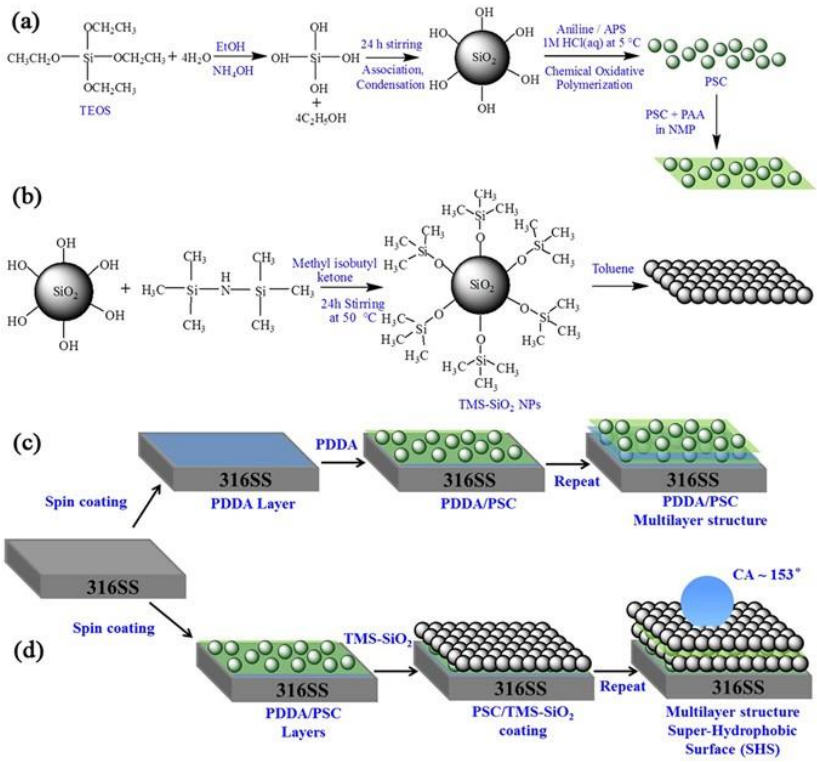

Figure 16. Schematic illustration of the synthesis of (**a**) PSC composite and preparation of its coating solution, (**b**) surface modification of silica to obtain TMS-SiO_2 NPs. Fabrication of (**c**) PDDA/PSC and (**d**) PSC/TMS-SiO_2 multilayers on 316SS by spin coating. Reproduced with permission from [116].

Amine functionalized polyethyleneimine multiwall carbon nanotubes (MW-CNTs-NH-PEI) were used in covalent or ionic LbL assembly to form nanocomposite thin films on functionalized polyethylene (PE) films. The surface exhibited a WSCA of 165° and sliding angle lower than 5°, while the surface produced by five ionic layer-by-layer deposition steps exhibited a water contact angle of 155° and water pinning. Depending on the assembly (ionic or covalent), the coating exhibited different durability and the covalently assembled one was identified to be more chemically robust [117].

Finally, A facile layer-by-layer deposition process for the deposition of transparent superhydrophobic coatings on glass was also reported by Yang Li et al. [118], yet the method can be applicable to metals.

4.7. Self-Healing Coatings

Despite the fact that there are reports about durable polymeric coatings and methods to improve their durability [15,41], most of the polymeric superhydrophobic and superamphiphobic coatings can be easily damaged by physical stress and this can lead to loss of the superhydrophobic properties. Therefore, although self-healing coatings can be fabricated by many methods, in this section we present indicative examples of self-healing coatings used mainly for corrosion protection of metals. In the review paper by Hughes et al. [119], metal protection schemes utilizing "green" inhibitors and "self-healing" paints are discussed. In particularly the authors discuss methods in encapsulation and polymer healing that can be used for the design of new protective paint systems.

A self-healing superamphiphobic coating for efficient corrosion protection of magnesium alloy, by the combination of a compact self-healing epoxy resin (SHEP) coating and a porous superamphiphobic coating, has been reported by Xia Zhao et al. [120]. The coating exhibited high contact angle, low sliding angle, robust impact/bounce behavior, excellent anticorrosion performance, and excellent self-healing performance. The authors concluded that the synergistic effect of the bi-layer structure was the reason for this optimized performance. In another example, self-healing coatings that can prevent corrosion of the underlying substrate are created through dispersion of microencapsulated healing agents in a polymer film. The approach was reported to be generic and applicable to both model and industrially important coatings [121].

In another work, different types of inhibitors were evaluated together with three different techniques for the application of the coatings [122]. The substrate was steel and the coatings were scribed and laboratory tested according to ASTM D 5894. It was found that if the coating compounds (primer, capsules with self-healing agent) were sprayed successively to form a three-layer coating (primer-capsules-primer), the performance was improved. Thus, it was concluded that the performance of some microcapsules was found to be dependent on the method of application.

Recently, an environment-friendly method with boiling water treatment and deposition of dopamine hydrochloride (DA) and hexadecyl trimethoxy silane (HDTMS) capsules on Al alloy was reported. The surfaces exhibited WSCA 155° and sliding angle lower than 5°, plus self-cleaning properties and corrosion resistance. The coating could also self-heal after heating [123]. The recent achievements in the field of self-healing coatings can be found in a dedicated review paper by Kobina Sam et al. [124].

5. Perspectives and Challenges

Superhydrophobicity as a tool to prevent corrosion and, hence, prolong the life span of metals and alloys is a well explored field [32]. The air which is retained on such surfaces can prevent corrosive processes (e.g., chloride ions in seawater from attacking the metal surface), offering a new efficient mechanism for anti-corrosion [125–127] Therefore, the idea of using superhydrophobicity for corrosion protection seems promising and can be expanded to many more functionalities that derive from wetting control.

To be applicable in real life applications, the fabrication technology should be low-cost, simple, and scalable, with a minimal environmental footprint. In this context, the first prerequisite towards realization of superhydrophobic metallic surfaces is the multiscale roughness. The second is to ensure a proper (low) surface energy, mostly via various engineered coatings or monolayers. The long-term stability of superhydrophobic surfaces under mechanical and thermal stress is a significant issue which should be addressed as well. In this review paper we reviewed the most common fabrication methods, employing both top-down and bottom-up approaches.

In the top-down methods, the wet chemical etching is considered as low-cost and scalable, but it is necessary to improve the binding/adhesion strength between the top hydrophobic coating used and the metal substrate. This technique also entails hazardous chemicals and is applicable mostly to specific metals such as aluminum and copper. Laser etching and plasma oxidation are dry subtractive methods with enormous potential in future applications as soon as the cost and scalability limitations are addressed.

On the hand, the durability of the bottom-up approaches relies on both the coating properties and the coating-substrate adhesion. Plasma deposition is a very promising technique, yet in many cases requires pre-roughening and it should; therefore, be combined with one of the top-down approaches. It is also critical to be performed in atmospheric pressure to be scalable and applicable to a wide range of material designs. To this direction, recent efforts have enabled the single-step deposition of textured hydrophobic coatings in continuous mode. The stability of atmospheric plasma-deposited superhydrophobic coatings should be drastically improved in the future for this technology to become more competitive. Spray coating is very simple, scalable, and versatile and it is already in use in

several industries, yet coating adhesion can be an issue in such efforts and the chemistries employed should be simple and environmental friendly. Sol–gel and layer-by-layer, in many cases, require even more complex chemistries compared to spraying and they should; therefore, become simpler for industrial adoption. The main bottleneck remains the poor durability of these coatings. Therefore, more studies or self-healing approaches should follow to address the poor mechanical durability of polymers compared to metals (In most of top-down approaches the topography is created on the metallic substrate and it is; therefore, more stable against mechanical stress). In Table 1 we outline selected literature findings employing both top-town and bottom-up approaches and we provide an assessment of the corresponding superhydrophobic properties.

Table 1. Representative works on superhydrophobic metallic surfaces.

Top Down Approaches			
Reference	**Substrate**	**Method/Category**	**Advantages/Wetting Properties**
[48]	Aluminum	Wet etching/subtractive	Chemical stability, mechanical durability, droplet impalement resistance. CA~160°, hysteresis < 10°
[50]	Aluminum	Wet etching/subtractive	Durability over time, environmentally friendly CA = 168.4 ± 3.1°, rolling angle = 0.5°
[51]	Aluminum	Wet etching/subtractive	Dropwise condensation, high heat transfer coefficient CA = ~150°, hysteresis < 10°
[52]	Aluminum	Wet etching/subtractive	Enhanced corrosion resistance, repellency against acidic and alkaline solutions CA = 150°, sliding angle < 10°
[53]	Aluminum, zinc	Wet etching/subtractive	Corrosion resistance. CA = 150°, roll-off angle ~8°
[55]	Copper	Wet etching/subtractive	Environmentally friendly method WSCA = 150°, sliding angle < 10°
[59]	Mg alloy	hydrothermal method	WSCA = 164° Rolling angle = 4°. Two times lower corrosion compared to the bare Mg alloy
[69]	Steel	Laser etching	Mechanical stability Scalability WSCA > 150°
[16]	Steel, titanium	Laser etching	Mechanical stability Scalability WSCA ~152°, hysteresis < 3°
[71]	Al, Cu and galvanized steel.	Laser etching	Superhydrophobicity with low sliding angles (0.5–3°) obtained for Cu and Al. Sliding angle for galvanized steel was relatively high although SWCA > 150°
[72]	Al and steel.	Laser etching	Surfaces repelled water, ethylene glycol, rapeseed oil, and cyclohexane and antifouling properties with good mechanical durability against abrasion
[128]	Titanium	Electrical discharged etching, wet etching	Mechanical stability in abrasion tests Corrosion resistance in NaCl solution
[63]	Aluminum	Oxidation	Mechanical stability after tape-peeling, and sandpaper-abrasion Chemical stability, corrosion resistance WSCA = 157.3° ± 0.5° Sliding angle = 3.6° ± 1°

Table 1. *Cont.*

[64]	Steel, magnesium	Oxidation	Mechanical durability at waterfall/jet test Steel: CA = 156.06°, SA = 2° Mg: CA = 152.65°, SA = 5°
Bottom-Up Approaches			
Reference	**Substrate**	**Method/Category**	**Advantages-Wetting Properties**
[24]	Aluminum	Synthesis	Mechanical stability, After abrasion test and sand-impact abrasion, the surface remained SH. WSCA = 164.8 ± 1.1°, sliding angle < 1°
[47]	Aluminum	Synthesis	One step method, environmentally friendly WSCA = 164°, HCA ~4°
[85]	Aluminum	Plasma coating	Durable in icing–de-icing cycles, Resistance to UV exposure, anticorrosion resistance WSCA = 162° ± 3°, sliding angle ~3°
[88]	Aluminum	Plasma coating	Durability for at least seven days when submerged into water, acid and base; durability in icing–de-icing cycles WSCA = 163°, sliding angle < 1°
[89]	Aluminum	Spray coating	Mechanical stability at high-pressure water jetting, sand particles impacting, and sandpaper shear abrasion tests WSCA = 155°, roll-off angle = 4°
[92]	Aluminum	Spray coating	Corrosion resistance for pH ranging 1–14 Mechanical stability after abrasion test and sand impacting WSCA = 159°, SA = 3.5°
[87]	Aluminum, copper	Plasma coating	Durability after storage in air or immersion in water for six months WSCA = 170°, Hysteresis: 5°
[91]	Copper	Spray coating	Anticorrosion resistance in NaCl solution, mechanical stability after adhesive tape test. WSCA = 156.9°, sliding angle < 5°
[73]	Magnesium	Electrodeposition	Anti-corrosion performance in NaCl solution WSCA > 158° and sliding angle < 2°
[74]	Magnesium	Electrodeposition	Anti-corrosion performance in NaCl solution, air exposure, droplets with pH ranging 1–13 WSCA > 158°, Sliding angle < 2°
[76]	Al alloy	Electrodeposition	WSCA 155° and 99.9% corrosion resistance when immersed inside a 3.5 wt% NaCl solution, even after 30 days of immersion
[82]	Magnesium	Plasma coating	Anticorrosion resistance, high chemical stability in neutral and acidic environments WSCA > 150°
[120]	Magnesium	Self-healing	Corrosion resistance in NaCl solution CA = 165.8° ± 2.1°, SA = 1° ± 0.6° at 3.5% wt NaCl droplet
[67]	Steel	Plasma synthesis	Corrosion resistance after 14 days in 5 wt% NaCl solution. WSCA > 160°, hysteresis ~4°
[84]	Steel	Plasma coating	Stable against moisture WSCA = 162°
[109]	Steel	Sol–gel	Durability at electrochemical and salt spray corrosion WSCA > 160°, hysteresis < 20°
[111]	Steel	Sol–gel	Corrosion resistance in NaCl solution, anti-corrosion ability in humid air at RH of 90% and 30 °C for 24 h WSCA = 158°, sliding angle = 2°

Table 1. *Cont.*

[116]	Steel	Layer-by-layer deposition	Corrosion resistance, after 240 h to 3.5% NaCl solution WSCA = 153° ± 2°, sliding angle = 6° ± 2°
[98]	Any metal	Electrospinning	WSCA = 163°, hysteresis = 15°
[100]	Any metal	Electrospinning	Good mechanical adhesion to fabrics WSCA = 158°, Roll-off angle ~5°
[101]	Any metal	Electrospinning	Applicability to any metal Industrial scalability WSCA > 160°, hysteresis < 10°
[117]	Any metal	Layer-by-layer deposition	Chemical stability WSCA = 165°, sliding angle < 5°
		Combination of the Two Approaches	
[60]	Aluminum	wet etching and synthesis	Chemical stability in acid and alkali solutions WSCA = 170.6 ± 2.0°, sliding angle 1.5 ± 1.0°
[61]	Aluminum	Wet etching and synthesis	Mechanical durability evaluated by the Scotch tape and hardness tests WSCA = 163°, sliding angle = 2°
[62]	Al	Anodization and liquid-phase deposition	Anticorrosion properties
[58]	Aluminum, titanium, steel, zinc, magnesium	Wet etching and synthesis	Corrosion resistance. Al: CA = 165°, RA ~4° Ti: CA = 165°, RA ~4° Steel: CA = 162°, RA ~7° Zn: CA = 160°, RA ~6° Mg: CA = 162°, RA ~2°
[54]	Copper	Wet etching and synthesis	Applicable also to other metals (zinc, silver), large scale applicability CA = 154°
[46]	Aluminum alloy AA6061	Wet etching and deposition	Superhydrophobicity WSCA ~162° Hysteresis ~4°.
[95]	Aluminum	Wet etching and sputtering	WSCA = 165 ± 2°, hysteresis: 5 ± 2°
[123]	Al alloy	Boiling water and deposition	WSCA 155° Sliding angle < 5°, self-healing and anticorrosion properties
[67]	Stainless Steel Sus 304	Plasma oxidation and deposition	WSCA 169° Anticorrosion properties after immersion inside a NaCl solution >2 weeks

Finally, it is worth noting that the evaluation of the surface properties should be done using specific protocols, such as ISO/TC 156 for the corrosion of metals and alloys, enabling, in this way, direct comparison of surfaces. We strongly believe that the extensive research in the field of wetting and interfacial phenomena and the constant development of technologies will solve the current drawbacks, and more artificial superhydrophobic surfaces will be applied in real life applications in the near future.

Author Contributions: K.E. and E.G.: Conceptualization, K.E.: Original Draft Preparation, K.E. and P.D.: writing, K.E., P.S. and P.D.: literature research., K.E., E.G. and P.D.: Review & Editing, K.E. & E.G.: Funding Acquisition. All authors have read and agreed to the published version of the manuscript.

Funding: This research is co-financed by Greece and the European Union (European Social Fund—ESF) through the Operational Programme «Human Resources Development, Education and Lifelong Learning» in the context of the project "Reinforcement of Postdoctoral Researchers—2nd Cycle" (MIS-5033021), implemented by the State Scholarships Foundation (IKΥ).

Institutional Review Board Statement: Not applicable.

Informed Consent Statement: Not applicable.

Conflicts of Interest: The authors declare no conflict of interest.

References

1. Nosonovsky, M.; Bhushan, B. Superhydrophobic surfaces and emerging applications: Non-adhesion, energy, green engineering. *Curr. Opin. Colloid Interface Sci.* **2009**, *14*, 270–280. [CrossRef]
2. Gao, X.; Yan, X.; Yao, X.; Xu, L.; Zhang, K.; Zhang, J.; Yang, B.; Jiang, L. The Dry-Style Antifogging Properties of Mosquito Compound Eyes and Artificial Analogues Prepared by Soft Lithography. *Adv. Mater.* **2007**, *19*, 2213–2217. [CrossRef]
3. Tzianou, M.; Thomopoulos, G.; Vourdas, N.; Ellinas, K.; Gogolides, E. Tailoring Wetting Properties at Extremes States to Obtain Antifogging Functionality. *Adv. Funct. Mater.* **2021**, *31*, 2006687. [CrossRef]
4. Yancheshme, A.A.; Momen, G.; Aminabadi, R.J. Mechanisms of ice formation and propagation on superhydrophobic surfaces: A review. *Adv. Colloid Interface Sci.* **2020**, *279*, 102155. [CrossRef]
5. Golovin, K.; Kobaku, S.P.R.; Lee, D.H.; DiLoreto, E.T.; Mabry, J.M.; Tuteja, A. Designing durable icephobic surfaces. *Sci. Adv.* **2016**, *2*, e1501496. [CrossRef]
6. Bayiati, P.; Malainou, A.; Matrozos, E.; Tserepi, A.; Petrou, P.S.; Kakabakos, S.E.; Gogolides, E. High-density protein patterning through selective plasma-induced fluorocarbon deposition on Si substrates. *Biosens. Bioelectron.* **2009**, *24*, 2979–2984. [CrossRef]
7. Fan, H.; Guo, Z. Bioinspired surfaces with wettability: Biomolecule adhesion behaviors. *Biomater. Sci.* **2020**, *8*, 1502–1535. [CrossRef] [PubMed]
8. Ellinas, K.; Kefallinou, D.; Stamatakis, K.; Gogolides, E.; Tserepi, A. Is There a Threshold in the Antibacterial Action of Superhydrophobic Surfaces? *ACS Appl. Mater. Interfaces* **2017**, *9*, 39781–39789. [CrossRef] [PubMed]
9. Kefallinou, D.; Ellinas, K.; Speliotis, T.; Stamatakis, K.; Gogolides, E.; Tserepi, A. Optimization of Antibacterial Properties of "Hybrid" Metal-Sputtered Superhydrophobic Surfaces. *Coatings* **2019**, *10*, 25. [CrossRef]
10. Dimitrakellis, P.; Ellinas, K.; Kaprou, G.D.; Mastellos, D.C.; Tserepi, A.; Gogolides, E. Bactericidal Action of Smooth and Plasma Micro-Nanotextured Polymeric Surfaces with Varying Wettability, Enhanced by Incorporation of a Biocidal Agent. *Macromol. Mater. Eng.* **2021**, 2000694. [CrossRef]
11. Pan, S.; Kota, A.K.; Mabry, J.M.; Tuteja, A. Superomniphobic Surfaces for Effective Chemical Shielding. *J. Am. Chem. Soc.* **2013**, *135*, 578–581. [CrossRef]
12. Zhu, Y.; Yang, F.; Guo, Z. Bioinspired surfaces with special micro-structures and wettability for drag reduction: Which surface design will be a better choice? *Nanoscale* **2021**, *13*, 3463–3482. [CrossRef]
13. Sarkiris, P.; Ellinas, K.; Gkiolas, D.; Mathioulakis, D.; Gogolides, E. Motion of Drops with Different Viscosities on Micro-Nanotextured Surfaces of Varying Topography and Wetting Properties. *Adv. Funct. Mater.* **2019**, *29*, 1902905. [CrossRef]
14. Brown, P.S.; Bhushan, B. Durable, superoleophobic polymer–nanoparticle composite surfaces with re-entrant geometry via solvent-induced phase transformation. *Sci. Rep.* **2016**, *6*, 21048. [CrossRef]
15. Ellinas, K.; Tserepi, A.; Gogolides, E. Durable superhydrophobic and superamphiphobic polymeric surfaces and their applications: A review. *Adv. Colloid Interface Sci.* **2017**, *250*, 132–157. [CrossRef] [PubMed]
16. Kietzig, A.-M.; Hatzikiriakos, S.G.; Englezos, P. Patterned Superhydrophobic Metallic Surfaces. *Langmuir* **2009**, *25*, 4821–4827. [CrossRef] [PubMed]
17. Mohamed, A.M.; Abdullah, A.M.; Younan, N.A. Corrosion behavior of superhydrophobic surfaces: A review. *Arab. J. Chem.* **2015**, *8*, 749–765. [CrossRef]
18. Chobaomsup, V.; Metzner, M.; Boonyongmaneerat, Y. Superhydrophobic surface modification for corrosion protection of metals and alloys. *J. Coat. Technol. Res.* **2020**, *17*, 583–595. [CrossRef]
19. Quan, Y.-Y.; Chen, Z.; Lai, Y.; Huang, Z.-S.; Li, H. Recent advances in fabricating durable superhydrophobic surfaces: A review in the aspects of structures and materials. *Mater. Chem. Front.* **2021**, *5*, 1655–1682. [CrossRef]
20. Yan, Y.; Gao, N.; Barthlott, W. Mimicking natural superhydrophobic surfaces and grasping the wetting process: A review on recent progress in preparing superhydrophobic surfaces. *Adv. Colloid Interface Sci.* **2011**, *169*, 80–105. [CrossRef]
21. Ellinas, K.; Tserepi, A.; Gogolides, E. From Superamphiphobic to Amphiphilic Polymeric Surfaces with Ordered Hierarchical Roughness Fabricated with Colloidal Lithography and Plasma Nanotexturing. *Langmuir* **2011**, *27*, 3960–3969. [CrossRef]
22. Ijaola, A.O.; Bamidele, E.A.; Akisin, C.J.; Bello, I.T.; Oyatobo, A.T.; Abdulkareem, A.; Farayibi, P.K.; Asmatulu, E. Wettability Transition for Laser Textured Surfaces: A Comprehensive Review. *Surf. Interfaces* **2020**, *21*, 100802. [CrossRef]
23. Tejero-Martin, D.; Rad, M.R.; McDonald, A.; Hussain, T. Beyond Traditional Coatings: A Review on Thermal-Sprayed Functional and Smart Coatings. *J. Therm. Spray Technol.* **2019**, *28*, 598–644. [CrossRef]

24. Zuo, Z.; Liao, R.; Guo, C.; Yuan, Y.; Zhao, X.; Zhuang, A.; Zhang, Y. Fabrication and anti-icing property of coral-like superhydrophobic aluminum surface. *Appl. Surf. Sci.* **2015**, *331*, 132–139. [CrossRef]
25. Cho, H.J.; Preston, D.J.; Zhu, Y.; Wang, E.N. Nanoengineered materials for liquid–vapour phase-change heat transfer. *Nat. Rev. Mater.* **2017**, *2*, 16092. [CrossRef]
26. Chen, Y.; Liu, J.; Song, J.; Liu, R.; Zhao, D.; Hua, S.; Lu, Y. Energy conversion based on superhydrophobic surfaces. *Phys. Chem. Chem. Phys.* **2020**, *22*, 25430–25444. [CrossRef] [PubMed]
27. Gogolides, E.; Ellinas, K.; Tserepi, A. Hierarchical micro and nano structured, hydrophilic, superhydrophobic and superoleophobic surfaces incorporated in microfluidics, microarrays and lab on chip microsystems. *Microelectron. Eng.* **2015**, *132*, 135–155. [CrossRef]
28. Dimitrakellis, P.; Gogolides, E. Hydrophobic and superhydrophobic surfaces fabricated using atmospheric pressure cold plasma technology: A review. *Adv. Colloid Interface Sci.* **2018**, *254*, 1–21. [CrossRef]
29. Ma, M.; Hill, R.M. Superhydrophobic surfaces. *Curr. Opin. Colloid Interface Sci.* **2006**, *11*, 193–202. [CrossRef]
30. Bai, Y.; Zhang, H.; Shao, Y.; Zhang, H.; Zhu, J. Recent Progresses of Superhydrophobic Coatings in Different Application Fields: An Overview. *Coatings* **2021**, *11*, 116. [CrossRef]
31. Yang, Y.; Xu, L.-P.; Zhang, X.; Wang, S. Bioinspired wettable–nonwettable micropatterns for emerging applications. *J. Mater. Chem. B* **2020**, *8*, 8101–8115. [CrossRef] [PubMed]
32. Vazirinasab, E.; Jafari, R.; Momen, G. Application of superhydrophobic coatings as a corrosion barrier: A review. *Surf. Coat. Technol.* **2018**, *341*, 40–56. [CrossRef]
33. Zhang, D.; Wang, L.; Qian, H.; Li, X. Superhydrophobic surfaces for corrosion protection: A review of recent progresses and future directions. *J. Coatings Technol. Res.* **2016**, *13*, 11–29. [CrossRef]
34. Peng, F.; Zhang, D.; Liu, X.; Zhang, Y. Recent progress in superhydrophobic coating on Mg alloys: A general review. *J. Magnes. Alloy.* **2021**. [CrossRef]
35. Darmanin, T.; De Givenchy, E.T.; Amigoni, S.; Guittard, F. Superhydrophobic Surfaces by Electrochemical Processes. *Adv. Mater.* **2013**, *25*, 1378–1394. [CrossRef]
36. Young, T., III. An essay on the cohesion of fluids. *Philos. Trans. R. Soc. Lond.* **1805**, *95*, 65–87. [CrossRef]
37. Hebbar, R.S.; Isloor, A.M.; Ismail, A.F. Contact Angle Measurements. In *Membrane Characterization*; Hilal, N., Matsuura, T., Oatley-Radcliffe, D., Fauzi Ismail, A., Eds.; Elsevier Inc.: Amsterdam, The Netherlands, 2017; Volume 122, pp. 219–255.
38. Bormashenko, E. Progress in understanding wetting transitions on rough surfaces. *Adv. Colloid Interface Sci.* **2015**, *222*, 92–103. [CrossRef]
39. Whyman, G.; Bormashenko, E.; Stein, T. The rigorous derivation of Young, Cassie–Baxter and Wenzel equations and the analysis of the contact angle hysteresis phenomenon. *Chem. Phys. Lett.* **2008**, *450*, 355–359. [CrossRef]
40. Johnson, R.E.; Dettre, R.H. Contact Angle Hysteresis. III. Study of an Idealized Heterogeneous Surface. *J. Phys. Chem.* **1964**, *68*, 1744–1750. [CrossRef]
41. Ellinas, K.; Pujari, S.P.; Dragatogiannis, D.A.; Charitidis, C.A.; Tserepi, A.; Zuilhof, H.; Gogolides, E. Plasma Micro-Nanotextured, Scratch, Water and Hexadecane Resistant, Superhydrophobic, and Superamphiphobic Polymeric Surfaces with Perfluorinated Monolayers. *ACS Appl. Mater. Interfaces* **2014**, *6*, 6510–6524. [CrossRef]
42. Marmur, A. The Lotus Effect: Superhydrophobicity and Metastability. *Langmuir* **2004**, *20*, 3517–3519. [CrossRef] [PubMed]
43. Bhushan, B.; Nosonovsky, M. The rose petal effect and the modes of superhydrophobicity. *Philos. Trans. R. Soc. A Math. Phys. Eng. Sci.* **2010**, *368*, 4713–4728. [CrossRef] [PubMed]
44. Sarkar, D.; Farzaneh, M.; Paynter, R. Superhydrophobic properties of ultrathin rf-sputtered Teflon films coated etched aluminum surfaces. *Mater. Lett.* **2008**, *62*, 1226–1229. [CrossRef]
45. Sarkar, D.K.; Farzaneh, M.; Paynter, R.W. Wetting and superhydrophobic properties of PECVD grown hydrocarbon and fluorinated-hydrocarbon coatings. *Appl. Surf. Sci.* **2010**, *256*, 3698–3701. [CrossRef]
46. Saleema, N.; Sarkar, D.K.; Paynter, R.W.; Chen, X.-G. Superhydrophobic Aluminum Alloy Surfaces by a Novel One-Step Process. *ACS Appl. Mater. Interfaces* **2010**, *2*, 2500–2502. [CrossRef]
47. Jafari, R.; Farzaneh, M. Fabrication of superhydrophobic nanostructured surface on aluminum alloy. *Appl. Phys. A* **2010**, *102*, 195–199. [CrossRef]
48. Maitra, T.; Antonini, C.; Der Mauer, M.A.; Stamatopoulos, C.; Tiwari, M.K.; Poulikakos, D. Hierarchically nanotextured surfaces maintaining superhydrophobicity under severely adverse conditions. *Nanoscale* **2014**, *6*, 8710–8719. [CrossRef]
49. Sharma, C.S.; Combe, J.; Giger, M.; Emmerich, T.; Poulikakos, D. Growth Rates and Spontaneous Navigation of Condensate Droplets Through Randomly Structured Textures. *ACS Nano* **2017**, *11*, 1673–1682. [CrossRef]
50. Song, J.; Xu, W.; Liu, X.; Lu, Y.; Wei, Z.; Wu, L. Ultrafast fabrication of rough structures required by superhydrophobic surfaces on Al substrates using an immersion method. *Chem. Eng. J.* **2012**, *211-212*, 143–152. [CrossRef]
51. Parin, R.; Martucci, A.; Sturaro, M.; Bortolin, S.; Bersani, M.; Carraro, F.; Del Col, D. Nano-structured aluminum surfaces for dropwise condensation. *Surf. Coat. Technol.* **2018**, *348*, 1–12. [CrossRef]
52. Lv, Z.; Yu, S.; Song, K.; Zhou, X.; Yin, X. A two-step method fabricating a hierarchical leaf-like superamphiphobic PTFE/CuO coating on 6061Al. *Prog. Org. Coat.* **2020**, *147*, 105723. [CrossRef]
53. Chen, C.; Yang, S.; Liu, L.; Xie, H.; Liu, H.; Zhu, L.; Xu, X. A green one-step fabrication of superhydrophobic metallic surfaces of aluminum and zinc. *J. Alloys Compd.* **2017**, *711*, 506–513. [CrossRef]

54. Song, W.; Zhang, J.; Xie, Y.; Cong, Q.; Zhao, B. Large-area unmodified superhydrophobic copper substrate can be prepared by an electroless replacement deposition. *J. Colloid Interface Sci.* **2009**, *329*, 208–211. [CrossRef]
55. Bahrami, H.R.T.; Ahmadi, B.; Saffari, H. Preparing superhydrophobic copper surfaces with rose petal or lotus leaf property using a simple etching approach. *Mater. Res. Express* **2017**, *4*, 055014. [CrossRef]
56. Liu, L.; Zhao, J.; Zhang, Y.; Zhao, F.; Zhang, Y. Fabrication of superhydrophobic surface by hierarchical growth of lotus-leaf-like boehmite on aluminum foil. *J. Colloid Interface Sci.* **2011**, *358*, 277–283. [CrossRef] [PubMed]
57. Nguyen, V.-H.; Nguyen, B.D.; Pham, H.T.; Lam, S.S.; Vo, D.-V.N.; Shokouhimehr, M.; Vu, T.H.H.; Nguyen, T.-B.; Kim, S.Y.; Van Le, Q. Anti-icing performance on aluminum surfaces and proposed model for freezing time calculation. *Sci. Rep.* **2021**, *11*, 1–9. [CrossRef] [PubMed]
58. Sun, J.; Chen, C.; Song, J.; Liu, J.; Yang, X.; Liu, J.; Liu, X.; Lu, Y. A universal method to create surface patterns with extreme wettability on metal substrates. *J. Colloid Interface Sci.* **2019**, *535*, 100–110. [CrossRef] [PubMed]
59. Chu, J.; Sun, G.; Tong, L.; Jiang, Z. Facile one-step hydrothermal fabrication of Allium giganteum-like superhydrophobic coating on Mg alloy with self-cleaning and anti-corrosion properties. *Colloids Surfaces A Physicochem. Eng. Asp.* **2021**, *617*, 126370. [CrossRef]
60. Zhang, B.; Zeng, Y.; Wang, J.; Sun, Y.; Zhang, J.; Li, Y. Superamphiphobic aluminum alloy with low sliding angles and acid-alkali liquids repellency. *Mater. Des.* **2020**, *188*, 108479. [CrossRef]
61. Barthwal, S.; Kim, Y.S.; Lim, S.-H. Mechanically Robust Superamphiphobic Aluminum Surface with Nanopore-Embedded Microtexture. *Langmuir* **2013**, *29*, 11966–11974. [CrossRef] [PubMed]
62. Rius-Ayra, O.; Llorca-Isern, N. A robust and anticorrosion non-fluorinated superhydrophobic aluminium surface for microplastic removal. *Sci. Total. Environ.* **2021**, *760*, 144090. [CrossRef]
63. Lv, Z.; Yu, S.; Song, K.; Zhou, X.; Yin, X. Fabrication of a leaf-like superhydrophobic CuO coating on 6061Al with good self-cleaning, mechanical and chemical stability. *Ceram. Int.* **2020**, *46*, 14872–14883. [CrossRef]
64. Wang, L.; Yang, J.; Zhu, Y.; Li, Z.; Shen, T.; Yang, D.-Q. An environment-friendly fabrication of superhydrophobic surfaces on steel and magnesium alloy. *Mater. Lett.* **2016**, *171*, 297–299. [CrossRef]
65. Mozetič, M.; Cvelbar, U.; Sunkara, M.K.; Vaddiraju, S. A Method for the Rapid Synthesis of Large Quantities of Metal Oxide Nanowires at Low Temperatures. *Adv. Mater.* **2005**, *17*, 2138–2142. [CrossRef]
66. Filipič, G.; Baranov, O.; Mozetic, M.; Ostrikov, K.; Cvelbar, U. Uniform surface growth of copper oxide nanowires in radiofrequency plasma discharge and limiting factors. *Phys. Plasmas* **2014**, *21*, 113506. [CrossRef]
67. Lee, E.; Lee, K.-H. Facile fabrication of superhydrophobic surfaces with hierarchical structures. *Sci. Rep.* **2018**, *8*, 1–7. [CrossRef]
68. Volpe, A.; Gaudiuso, C.; Ancona, A. Laser Fabrication of Anti-Icing Surfaces: A Review. *Materials* **2020**, *13*, 5692. [CrossRef]
69. Samanta, A.; Wang, Q.; Shaw, S.K.; Ding, H. Nanostructuring of laser textured surface to achieve superhydrophobicity on engineering metal surface. *J. Laser Appl.* **2019**, *31*, 022515. [CrossRef]
70. Raja, R.S.S.; Selvakumar, P.; Babu, P.D. A novel fabrication of superhydrophobic surfaces on aluminium substrate by picosecond pulsed laser. *J. Mech. Sci. Technol.* **2020**, *34*, 1667–1674. [CrossRef]
71. Khan, S.A.; Boltaev, G.S.; Iqbal, M.; Kim, V.; Ganeev, R.A.; Alnaser, A.S. Ultrafast fiber laser-induced fabrication of superhydrophobic and self-cleaning metal surfaces. *Appl. Surf. Sci.* **2021**, *542*, 148560. [CrossRef]
72. Tuo, Y.; Zhang, H.; Chen, L.; Chen, W.; Liu, X.; Song, K. Fabrication of superamphiphobic surface with hierarchical structures on metal substrate. *Colloids Surfaces A Physicochem. Eng. Asp.* **2021**, *612*, 125983. [CrossRef]
73. Zhang, B.; Zhu, Q.; Li, Y.; Hou, B. Facile fluorine-free one step fabrication of superhydrophobic aluminum surface towards self-cleaning and marine anticorrosion. *Chem. Eng. J.* **2018**, *352*, 625–633. [CrossRef]
74. Liu, X.; Zhang, T.C.; He, H.; Ouyang, L.; Yuan, S. A stearic Acid/CeO2 bilayer coating on AZ31B magnesium alloy with superhydrophobic and self-cleaning properties for corrosion inhibition. *J. Alloys Compd.* **2020**, *834*, 155210. [CrossRef]
75. Zhao, N.; Shi, F.; Wang, Z.; Zhang, X. Combining Layer-by-Layer Assembly with Electrodeposition of Silver Aggregates for Fabricating Superhydrophobic Surfaces. *Langmuir* **2005**, *21*, 4713–4716. [CrossRef] [PubMed]
76. He, Z.; Zeng, Y.; Zhou, M.; Min, Y.; Shen, X.; Xu, Q. Superhydrophobic Films with Enhanced Corrosion Resistance and Self-Cleaning Performance on an Al Alloy. *Langmuir* **2021**, *37*, 524–541. [CrossRef]
77. Alam, M.A.; Sherif, E.-S.M.; Al-Zahrani, S.M. Fabrication of various epoxy coatings for offshore applications and evaluating their mechanical properties and corrosion behavior. *Int. J. Electrochem. Sci.* **2013**, *8*, 3121–3131.
78. Bakhshandeh, E.; Jannesari, A.; Ranjbar, Z.; Sobhani, S.; Saeb, M.R. Anti-corrosion hybrid coatings based on epoxy–silica nano-composites: Toward relationship between the morphology and EIS data. *Prog. Org. Coat.* **2014**, *77*, 1169–1183. [CrossRef]
79. Dimitrakellis, P.; Gogolides, E. Atmospheric plasma etching of polymers: A palette of applications in cleaning/ashing, pattern formation, nanotexturing and superhydrophobic surface fabrication. *Microelectron. Eng.* **2018**, *194*, 109–115. [CrossRef]
80. Dimitrakellis, P.; Patsidis, A.; Smyrnakis, A.; Psarras, G.; Gogolides, E. Atmospheric Plasma Nanotexturing of Organic–Inorganic Nanocomposite Coatings for Multifunctional Surface Fabrication. *ACS Appl. Nano Mater.* **2019**, *2*, 2969–2978. [CrossRef]
81. Grundmeier, G.; Thiemann, P.; Carpentier, J.; Shirtcliffe, N.; Stratmann, M. Tailoring of the morphology and chemical composition of thin organosilane microwave plasma polymer layers on metal substrates. *Thin Solid Films* **2004**, *446*, 61–71. [CrossRef]
82. Ishizaki, T.; Hieda, J.; Saito, N.; Saito, N.; Takai, O. Corrosion resistance and chemical stability of super-hydrophobic film deposited on magnesium alloy AZ31 by microwave plasma-enhanced chemical vapor deposition. *Electrochimica Acta* **2010**, *55*, 7094–7101. [CrossRef]

83. Beck, A.; Short, R.; Matthews, A. Deposition of functional coatings from acrylic acid and octamethylcyclotetrasiloxane onto steel using an atmospheric pressure dielectric barrier discharge. *Surf. Coatings Technol.* **2008**, *203*, 822–825. [CrossRef]
84. Kim, M.; Klages, C.-P. One-step process to deposit a soft super-hydrophobic film by filamentary dielectric barrier discharge-assisted CVD using HMCTSO as a precursor. *Surf. Coat. Technol.* **2009**, *204*, 428–432. [CrossRef]
85. Mobarakeh, L.F.; Jafari, R.; Farzaneh, M. Robust icephobic, and anticorrosive plasma polymer coating. *Cold Reg. Sci. Technol.* **2018**, *151*, 89–93. [CrossRef]
86. Boscher, N.D.; Duday, D.; Verdier, S.; Choquet, P. Single-Step Process for the Deposition of High Water Contact Angle and High Water Sliding Angle Surfaces by Atmospheric Pressure Dielectric Barrier Discharge. *ACS Appl. Mater. Interfaces* **2013**, *5*, 1053–1060. [CrossRef] [PubMed]
87. Boscher, N.D.; Vaché, V.; Carminati, P.; Grysan, P.; Choquet, P. A simple and scalable approach towards the preparation of superhydrophobic surfaces–importance of the surface roughness skewness. *J. Mater. Chem. A* **2014**, *2*, 5744–5750. [CrossRef]
88. Jafari, R.; Momen, G.; Eslami, E. Fabrication of icephobic aluminium surfaces by atmospheric plasma jet polymerisation. *Surf. Eng.* **2019**, *35*, 450–455. [CrossRef]
89. Zhang, Y.; Ge, D.; Yang, S. Spray-coating of superhydrophobic aluminum alloys with enhanced mechanical robustness. *J. Colloid Interface Sci.* **2014**, *423*, 101–107. [CrossRef] [PubMed]
90. Li, J.; Wu, R.; Jing, Z.; Yan, L.; Zha, F.; Lei, Z. One-Step Spray-Coating Process for the Fabrication of Colorful Superhydrophobic Coatings with Excellent Corrosion Resistance. *Langmuir* **2015**, *31*, 10702–10707. [CrossRef]
91. El Dessouky, W.I.; Abbas, R.; Sadik, W.A.; El Demerdash, A.G.M.; Hefnawy, A. Improved adhesion of superhydrophobic layer on metal surfaces via one step spraying method. *Arab. J. Chem.* **2017**, *10*, 368–377. [CrossRef]
92. Wang, H.; Zhang, X.; Liu, Z.; Zhu, Y.; Wu, S.; Zhu, Y. A superrobust superhydrophobic PSU composite coating with self-cleaning properties, wear resistance and corrosion resistance. *RSC Adv.* **2016**, *6*, 10930–10937. [CrossRef]
93. Wang, S.; Zhang, W.; Yu, X.; Liang, C.; Zhang, Y. Sprayable superhydrophobic nano-chains coating with continuous self-jumping of dew and melting frost. *Sci. Rep.* **2017**, *7*, 40300. [CrossRef] [PubMed]
94. Wu, W.; Wang, X.; Liu, X.; Zhou, F. Spray-Coated Fluorine-Free Superhydrophobic Coatings with Easy Repairability and Applicability. *ACS Appl. Mater. Interfaces* **2009**, *1*, 1656–1661. [CrossRef]
95. Wang, Y.; Liu, X.W.; Zhang, H.F.; Zhou, Z.P. Fabrication of super-hydrophobic surfaces on aluminum alloy substrates by RF-sputtered polytetrafluoroethylene coatings. *AIP Adv.* **2014**, *4*, 031323. [CrossRef]
96. Lu, X.; Wang, C.; Wei, Y. One-Dimensional Composite Nanomaterials: Synthesis by Electrospinning and Their Applications. *Small* **2009**, *5*, 2349–2370. [CrossRef]
97. Cui, M.; Xu, C.; Shen, Y.; Tian, H.; Feng, H.; Li, J. Electrospinning superhydrophobic nanofibrous poly(vinylidene fluoride)/stearic acid coatings with excellent corrosion resistance. *Thin Solid Films* **2018**, *657*, 88–94. [CrossRef]
98. Ma, M.; Hill, R.M.; Lowery, J.L.; Fridrikh, S.V.; Rutledge, G.C. Electrospun Poly(Styrene-block-dimethylsiloxane) Block Copolymer Fibers Exhibiting Superhydrophobicity. *Langmuir* **2005**, *21*, 5549–5554. [CrossRef]
99. Ma, M.; Mao, Y.; Gupta, M.; Gleason, K.K.; Rutledge, G.C. Superhydrophobic Fabrics Produced by Electrospinning and Chemical Vapor Deposition. *Macromolecules* **2005**, *38*, 9742–9748. [CrossRef]
100. Han, D.; Steckl, A.J. Superhydrophobic and Oleophobic Fibers by Coaxial Electrospinning. *Langmuir* **2009**, *25*, 9454–9462. [CrossRef] [PubMed]
101. Alqadhi, M.; Merah, N.; Matin, A.; Abu-Dheir, N.; Khaled, M.; Youcef-Toumi, K. Preparation of superhydrophobic and self-cleaning polysulfone non-wovens by electrospinning: Influence of process parameters on morphology and hydrophobicity. *J. Polym. Res.* **2015**, *22*, 1–9. [CrossRef]
102. Acatay, K.; Simsek, E.; Ow-Yang, C.; Menceloglu, Y.Z. Tunable, Superhydrophobically Stable Polymeric Surfaces by Electrospinning. *Angew. Chem. Int. Ed.* **2004**, *43*, 5210–5213. [CrossRef]
103. Hardman, S.J.; Muhamad-Sarih, N.; Riggs, H.J.; Thompson, R.L.; Rigby, J.; Bergius, W.N.A.; Hutchings, L.R. Electrospinning Superhydrophobic Fibers Using Surface Segregating End-Functionalized Polymer Additives. *Macromolecules* **2011**, *44*, 6461–6470. [CrossRef]
104. Lamaka, S.; Montemor, M.; Galio, A.; Zheludkevich, M.; Trindade, C.; Dick, L.; Ferreira, M. Novel hybrid sol–gel coatings for corrosion protection of AZ31B magnesium alloy. *Electrochimica Acta* **2008**, *53*, 4773–4783. [CrossRef]
105. Guglielmi, M. Sol-Gel Coatings on Metals. *J. Sol-Gel Sci. Technol.* **1997**, *8*, 443–449. [CrossRef]
106. Wang, D.; Bierwagen, G.P. Sol–gel coatings on metals for corrosion protection. *Prog. Org. Coat.* **2009**, *64*, 327–338. [CrossRef]
107. Mahadik, S.A.; Mahadik, D.B.; Kavale, M.S.; Parale, V.G.; Wagh, P.B.; Barshilia, H.C.; Gupta, S.C.; Hegde, N.D.; Rao, A.V. Thermally stable and transparent superhydrophobic sol–gel coatings by spray method. *J. Sol Gel Sci. Technol.* **2012**, *63*, 580–586. [CrossRef]
108. Lu, S.; Chen, Y.; Xu, W.; Liu, W. Controlled growth of superhydrophobic films by sol–gel method on aluminum substrate. *Appl. Surf. Sci.* **2010**, *256*, 6072–6075. [CrossRef]
109. Arukalam, I.O.; Oguzie, E.E.; Li, Y. Nanostructured superhydrophobic polysiloxane coating for high barrier and anticorrosion applications in marine environment. *J. Colloid Interface Sci.* **2018**, *512*, 674–685. [CrossRef] [PubMed]
110. Zheng, S.; Li, J. Inorganic–organic sol gel hybrid coatings for corrosion protection of metals. *J. Sol-Gel Sci. Technol.* **2010**, *54*, 174–187. [CrossRef]

111. Wang, N.; Xiong, D. Superhydrophobic membranes on metal substrate and their corrosion protection in different corrosive media. *Appl. Surf. Sci.* **2014**, *305*, 603–608. [CrossRef]
112. Barkhudarov, P.M.; Shah, P.B.; Watkins, E.B.; Doshi, D.A.; Brinker, C.J.; Majewski, J. Corrosion inhibition using superhydrophobic films. *Corros. Sci.* **2008**, *50*, 897–902. [CrossRef]
113. Chen, W.; McCarthy, T.J. Layer-by-Layer Deposition: A Tool for Polymer Surface Modification. *Macromolecules* **1997**, *30*, 78–86. [CrossRef]
114. Zhang, X.; Chen, H.; Zhang, H. Layer-by-layer assembly: From conventional to unconventional methods. *Chem. Commun.* **2007**, 1395–1405. [CrossRef] [PubMed]
115. Richardson, J.J.; Bjornmalm, A.M.H.; Caruso, F. Technology-driven layer-by-layer assembly of nanofilms. *Science* **2015**, *348*, aaa2491. [CrossRef] [PubMed]
116. Syed, J.A.; Tang, S.; Meng, X. Super-hydrophobic multilayer coatings with layer number tuned swapping in surface wettability and redox catalytic anti-corrosion application. *Sci. Rep.* **2017**, *7*, 1–17. [CrossRef] [PubMed]
117. Liao, K.-S.; Wan, A.; Batteas, A.J.D.; Bergbreiter, D.E. Superhydrophobic Surfaces Formed Using Layer-by-Layer Self-Assembly with Aminated Multiwall Carbon Nanotubes. *Langmuir* **2008**, *24*, 4245–4253. [CrossRef] [PubMed]
118. Li, Y.; Liu, F.; Sun, J. A facile layer-by-layer deposition process for the fabrication of highly transparent superhydrophobic coatings. *Chem. Commun.* **2009**, 2730–2732. [CrossRef]
119. Hughes, A.E.; Cole, I.S.; Muster, T.H.; Varley, R.J. Designing green, self-healing coatings for metal protection. *NPG Asia Mater.* **2010**, *2*, 143–151. [CrossRef]
120. Zhao, X.; Wei, J.; Li, B.; Li, S.; Tian, N.; Jing, L.; Zhang, J. A self-healing superamphiphobic coating for efficient corrosion protection of magnesium alloy. *J. Colloid Interface Sci.* **2020**, *575*, 140–149. [CrossRef]
121. Cho, S.H.; White, S.R.; Braun, P.V. Self-Healing Polymer Coatings. *Adv. Mater.* **2009**, *21*, 645–649. [CrossRef]
122. Kumar, A.; Stephenson, L.; Murray, J. Self-healing coatings for steel. *Prog. Org. Coat.* **2006**, *55*, 244–253. [CrossRef]
123. Zhang, Z.; Xue, F.; Bai, W.; Shi, X.; Liu, Y.; Feng, L. Superhydrophobic surface on Al alloy with robust durability and excellent self-healing performance. *Surf. Coat. Technol.* **2021**, *410*, 126952. [CrossRef]
124. Sam, E.K.; Sam, D.K.; Lv, X.; Liu, B.; Xiao, X.; Gong, S.; Yu, W.; Chen, J.; Liu, J. Recent development in the fabrication of self-healing superhydrophobic surfaces. *Chem. Eng. J.* **2019**, *373*, 531–546. [CrossRef]
125. Liu, T.; Chen, S.; Cheng, S.; Tian, J.; Chang, X.; Yin, Y. Corrosion behavior of super-hydrophobic surface on copper in seawater. *Electrochim. Acta* **2007**, *52*, 8003–8007. [CrossRef]
126. Yin, Y.; Liu, T.; Chen, S.; Liu, T.; Cheng, S. Structure stability and corrosion inhibition of super-hydrophobic film on aluminum in seawater. *Appl. Surf. Sci.* **2008**, *255*, 2978–2984. [CrossRef]
127. Zhang, F.; Zhao, L.; Chen, H.; Xu, S.; Evans, D.G.; Duan, X. Corrosion Resistance of Superhydrophobic Layered Double Hydroxide Films on Aluminum. *Angew. Chem. Int. Ed.* **2008**, *47*, 2466–2469. [CrossRef]
128. Dong, S.; Wang, Z.; An, L.; Li, Y.; Wang, B.; Ji, H.; Wang, H. Facile Fabrication of a Superhydrophobic Surface with Robust Micro-/Nanoscale Hierarchical Structures on Titanium Substrate. *Nanomaterials* **2020**, *10*, 1509. [CrossRef] [PubMed]